8-Alkynyl-3-nitroimidazopyridines display potent antitrypanosomal activity against both T. b. brucei and cruzi

Fersing, Cyril; Boudot, Clotilde; Castera-Ducros, Caroline; Pinault, Emilie; Hutter, Sébastien; Paoli-Lombardo, Romain

Published in:
European Journal of Medicinal Chemistry

DOI:
10.1016/j.ejmech.2020.112558

Publication date:
2020

Author Accepted Manuscript: Fersing, Cyril et al. "8-Alkynyl-3-nitroimidazopyridines display potent antitrypanosomal activity against both T. b. brucei and cruzi". European Journal of Medicinal Chemistry. 2020. 202. https://doi.org/10.1016/j.ejmech.2020.112558

8-Alkynyl-3-nitroimidazopyridines display potent antitrypanosomal activity against both *T. b. brucei* and *cruzi*

Cyril Fersing[1#], Clotilde Boudot[2#], Caroline Castera-Ducros[1], Emilie Pinault[3], Sébastien Hutter[4], Romain Paoli-Lombardo[1], Nicolas Primas[1], Julien Pedron[5], Line Seguy[5], Sandra Bourgeade-Delmas[6], Alix Sournia-Saquet[5], Jean-Luc Stigliani[5], Jean-Yves Brossas[7], Luc Paris[7], Alexis Valentin[6], Susan Wyllie[8], Alan H. Fairlamb[8], Élisa Boutet-Robinet[9], Sophie Corvaisier[10], Marc Since[10], Aurélie Malzert-Fréon[10], Alexandre Destere[11], Dominique Mazier[12], Pascal Rathelot[1], Bertrand Courtioux[2], Nadine Azas[4], Pierre Verhaeghe[5*] and Patrice Vanelle[1].

[1] Aix Marseille Univ, CNRS, ICR UMR 7273, Equipe Pharmaco-Chimie Radicalaire, Faculté de Pharmacie, 27 Boulevard Jean Moulin, CS30064, 13385, Marseille Cedex 05, France.

[2] Université de Limoges, UMR Inserm 1094, Neuroépidémiologie Tropicale, Faculté de Pharmacie, 2 rue du Dr Marcland, 87025 Limoges, France.

[3] Université de Limoges, BISCEm Mass Spectrometry Platform, CBRS, 2 rue du Pr. Descottes, F-87025 Limoges, France.

[4] Aix Marseille Univ, IHU Méditerranée Infection, UMR VITROME - Tropical Eukaryotic Pathogens, 19-21 Boulevard Jean Moulin, 13005 Marseille, France.

[5] LCC-CNRS Université de Toulouse, CNRS, UPS, Toulouse, France.

[6] UMR 152 PHARMA-DEV, Université de Toulouse, IRD, UPS, Toulouse, France.

[7] AP-HP, Groupe Hospitalier Pitié-Salpêtrière, Service de Parasitologie Mycologie, Paris, France.

[8] University of Dundee, School of Life Sciences, Division of Biological Chemistry and Drug Discovery, Dow Street, Dundee DD1 5EH, Scotland, United Kingdom.

[9] Toxalim (Research Centre in Food Toxicology), Université de Toulouse, INRA, ENVT, INP-Purpan, UPS, Toulouse, France.

[10] Normandie Univ, UNICAEN, CERMN, 14000 Caen, France

[11] Department of Pharmacology, Toxicology and Pharmacovigilance, CHU Limoges, Limoges, France, INSERM, UMR 1248, University of Limoges, France.

[12] CIMI-Paris, Sorbonne Université 91 boulevard de l'Hôpital 75013 Paris, France.

[#]Co first-authors

[*]Corresponding author:
E-mail address: pierre.verhaeghe@lcc-toulouse.fr (P. Verhaeghe)
Postal address: Université Paul Sabatier, Faculté des Sciences Pharmaceutiques - CNRS UPR 8241, Laboratoire de Chimie de Coordination, 205 Route de Narbonne, 31077 Toulouse cedex 04, France.

Abstract:

An antikinetoplastid pharmacomodulation study was done at position 8 of a previously identified pharmacophore in 3-nitroimidazo[1,2-*a*]pyridine series. Twenty original derivatives bearing an alkynyl moiety were synthesized *via* a Sonogashira cross-coupling reaction and tested *in vitro*, highlighting 3 potent (40 nM ≤ EC_{50} blood stream form≤ 70 nM) and selective (500 ≤ SI ≤ 1800) anti-*T. brucei brucei* molecules (**19**, **21** and **22**), in comparison with four reference drugs. Among these hit molecules, compound **19** also showed the same level of activity against *T. cruzi* (EC_{50} amastigotes = 1.2 µM) as benznidazole and fexinidazole. An *in vitro* comet assay showed that nitroaromatic derivative **19** was not genotoxic. It displayed a low redox potential value (-0.68 V/NHE) and was shown to be bioactivated by type 1 nitroreductases both in *Leishmania* and *Trypanosoma*. The SAR study indicated that an alcohol function improved aqueous solubility while maintaining good activity and low cytotoxicity when the hydroxyl group was at position *beta* of the alkyne triple bond. Hit-compound **19** was also evaluated regarding *in vitro* pharmacokinetic data: **19** is BBB permeable (PAMPA assay), has a 16 min microsomal half-life and a high albumin binding (98.5%). Moreover, compound **19** was orally absorbed and was well tolerated in mouse after both single and repeated administrations at 100 mg/kg. Its mouse plasma half-life (10 h) is also quite encouraging, paving the way toward further efficacy evaluations in parasitized mouse models, looking for a novel antitrypanosomal lead compound.

Keywords: Imidazo[1,2-*a*]pyridine; Nitroaromatic; Nitroreductases; Kinetoplastids; Comet assay; SARs.

1. Introduction

Neglected tropical diseases (NTDs) constitute a heterogeneous group of communicable diseases that occur mainly in developing countries and are closely related to poverty [1]. Among the 20 NTDs listed to date by the WHO, three are caused by trypanosomatid protozoa: leishmaniasis (caused by several *Leishmania* species) [2], human African trypanosomiasis (HAT, consequence of an infection by *Trypanosoma brucei*) [3] and Chagas disease (CD, related to an infection by *Trypanosoma cruzi*) [4]. Half a billion people, mainly in tropical and sub-tropical areas, are at risk of contracting one of these 3 NTDs. The number of individuals infected with these pathogens is estimated at nearly 20 million, causing up to 50,000 deaths per year [5]. Moreover, it is very likely that these values are underestimated due to difficulties in data collection in the most rural and isolated areas. In the absence of human vaccines or chemoprophylaxis to prevent the transmission of these parasitic diseases in human, the control of trypanosomatid infections relies on eradication of vectors, management of animal reservoirs and chemotherapy. Only a small number of molecules are currently available as antitrypanosomatid treatments, most of them associated with significant drawbacks such as a lack of efficacy, toxicities, constraining dosing regimens or non-oral route of administration. Likewise, very few new chemical entities have currently reached the clinical stage of development, even if significant results have been achieved in the treatment of HAT since the marketing authorization of the nitroaromatic drug fexinidazole in 2018 (**Figure 1**) [6]. Thus, there are currently only three new antileishmanial drugs in clinical trials according to DNDi, all being studied in the early phase 1 [7]. Regarding sleeping sickness, only acoziborole remains in phase IIb/III clinical trial and, more worryingly, no original anti-*Trypanosoma cruzi* molecule is under evaluation in humans at this time, despite major needs. Only fexinidazole is currently used in a phase II proof-of-concept study as a possible treatment of Chagas disease. Thus, efficient, safe and cheap orally available antikinetoplastid agents are awaited [8], particularly against VL and CD [9], considering both mortality but also the genotoxic character of the two molecules used against CD: nifurtimox and benznidazole [10]. Nevertheless, nitroaromatic derivatives are a major group of

antikinetoplastid molecules (**Figure 1**) and the recent introduction of fexinidazole (a non-genotoxic 5-nitroimidazole derivative) as an oral drug for the treatment of HAT is certainly a pivotal milestone [6] which illustrates the interest of developing novel nitroheterocyclic drugs to fight against trypanosomatid infections [11]. In general, anti-infective nitroheterocycles act as prodrugs requiring a bioactivation step [12]. The accepted mechanism of action for these compounds involves, first of all, their entry into the parasite by passive diffusion, their reduction into various reactive metabolites (nitroso, hydroxylamine), and finally the reaction of these electrophilic metabolites with cellular components such as DNA or proteins, to form covalent adducts that are cytotoxic [13].

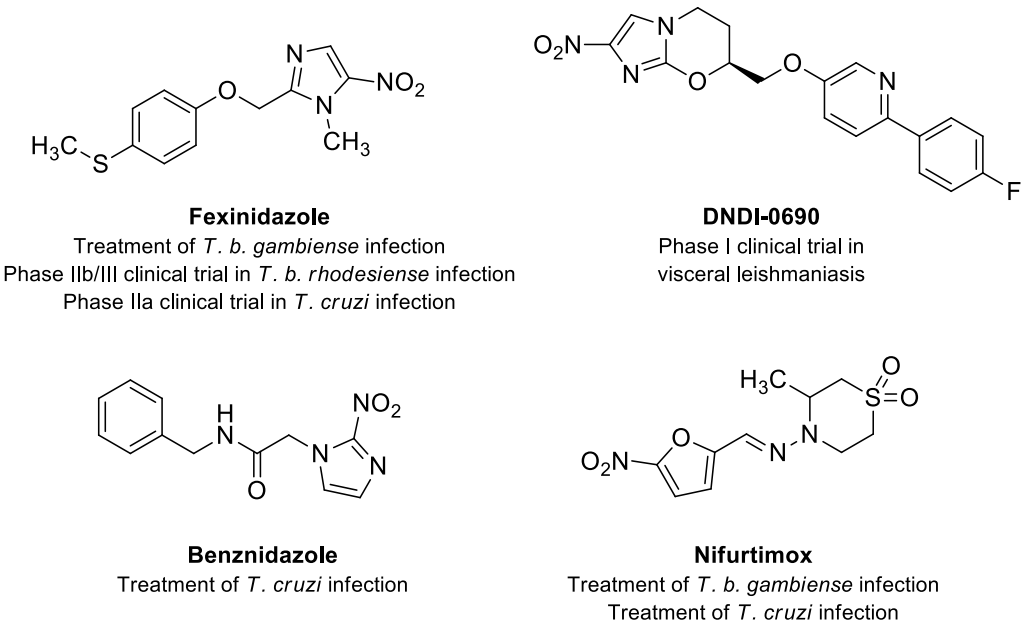

Figure 1. Structures of nitroheterocyclic drug-compounds used in the treatments of trypanosomatid infections.

The enzymes catalyzing nitrodrugs activation are nitroreductases (NTRs). Two NTRs have been identified in *Leishmania* (mitochondrial type 1 NTR1 [14], responsible for the activation of 5-nitroimidazoles such as fexinidazole [15,16]; and cytosolic type 2 NTR2 [17], responsible for the activation of bicyclic nitroheterocycles such as delamanid or pretomanid [18]), whereas only one NTR was discovered in *Trypanosoma* (type 1 NTR, initiating the activation of nifurtimox [19] and

benznidazole [20]). As NTRs are absent from mammalian cells, substrates of these enzymes can be envisaged as selective antikinetoplastid candidates. Unfortunately, no X-ray structure of parasitic NTRs was reported and their low degree of homology with bacterial isoforms restricts the use of most classical rational medicinal chemistry approaches, such as molecular docking, for the design of new nitrodrug substrates of these enzymes.

Looking for original nitroheterocyclic antikinetoplastid molecules, our group formerly identified a first antileishmanial hit molecule in 8-halogeno-3-nitroimidazo[1,2-*a*]pyridine series (hit **A**, **Figure 2**) [21]. Subsequent work demonstrated the key role of the substituent in position 8 of the scaffold. Introduction of an heteroaryl moiety in this position improved *in vitro* activity against *Trypanosoma b. brucei* but was not satisfying regarding water solubility (hit **B**, **Figure 2**) [22]. Introduction of a phenylthio moiety at position 8 slightly improved *in vitro* antileishmanial activity and aqueous solubility (hit **C**, **Figure 2**) [23]. Nevertheless, hit-compound **C** showed a poor mouse liver microsomal stability ($T_{1/2}$ = 3 min). Then, in a view to improve both antitrypanosomal activity and microsomal stability of this series, we present herein the benefit of introducing a hydroxyalkynyl group at position 8 of the 3-nitroimidazo[1,2-*a*]pyridine scaffold, using the Sonogashira cross-coupling reaction.

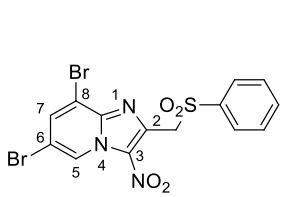

Initial hit molecule **A**

EC_{50} *L. donovani* intramacro. ama.	5.5 µM
EC_{50} *T. brucei brucei* BSF	2.9 µM
CC_{50} HepG2	>31 µM
CC_{50} THP1	>25 µM
Microsomal half-life	9 min

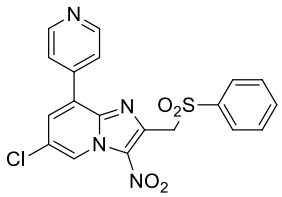

Optimized hit molecule **B**

EC_{50} *L. donovani* intramacro. ama.	2.3 µM
EC_{50} *T. brucei brucei* trypo.	0.25 µM
CC_{50} HepG2	>50 µM
CC_{50} THP1	>25 µM

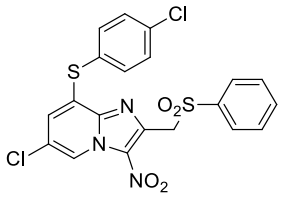

Optimized hit molecule **C**

EC_{50} *L. donovani* intramacro. ama.	1.3 µM
EC_{50} *T. brucei brucei* trypo.	1.3 µM
CC_{50} HepG2	>100 µM
CC_{50} THP1	>62.5 µM
Microsomal half-life	3 min

Figure 2. Structures and biological profiles of previously identified antikinetoplastid hit-compounds in 3-nitroimidazo[1,2-*a*]pyridine series [21-23].

2. Results and discussion

The substrate 8-bromo-6-chloro-3-nitro-2-(phenylsulfonylmethyl)imidazo[1,2-*a*]pyridine **4** was prepared in four steps as previously described [22]. The use of the Sonogashira cross-coupling reaction for the antitrypanosomatid pharmacomodulation of a nitroaromatic scaffold is an interesting option that was already reported by our team [24]. Hence, the Sonogashira reaction conditions were optimized from previously described protocols [25-26] to afford 20 original 8-alkynylimidazo[1,2-*a*]pyridine derivatives (**Scheme 1**). Primary alkyne reagents were chosen to display a large panel of lipophilicity and flexibility, varying from rigid and highly lipophilic aromatic derivatives to more flexible and hydrophilic hydroxyaliphatic derivatives. Coupling products were isolated with moderate to good yields (30–90%). Finally, the reduction of the nitro group of **19** afforded the amino derivative **25**, considered as a negative control.

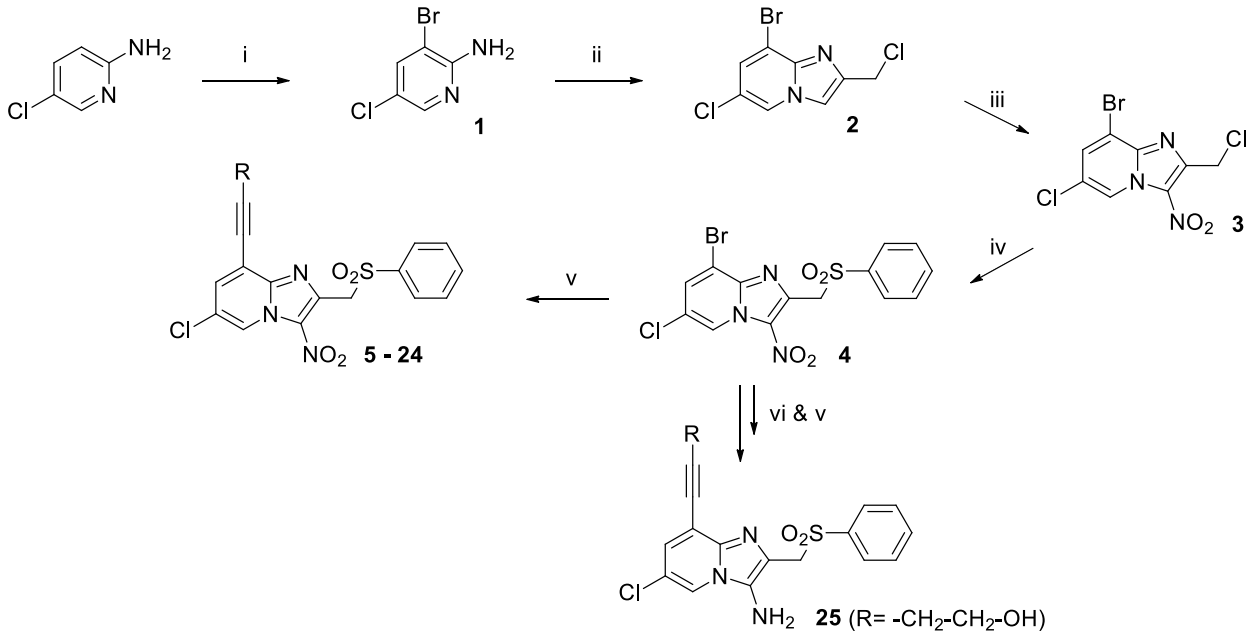

Scheme 1. Synthesis of compounds **1-25**.

Reagents and conditions: (i) NBS 1 equiv, ACN, 80°C, 1 h, 71%; (ii) 1,3-dichloroacetone 1.1 equiv, EtOH, 80°C, 96 h, 60%; (iii) HNO_3 6 equiv, H_2SO_4, 0°C→RT, 1 h, 60%; (iv) Sodium benzenesulfinate 3 equiv, DMSO, RT, 3 h, 80%. (v) appropriate alkyne 1.5 equiv, $Pd(PPh_3)_4$ 0.1

equiv, CuI 0.1 equiv, diisopropylamine 12 equiv, THF, RT, 1 to 24 h, 30% to 90%. (vi) Fe 10 equiv, AcOH, reflux, 30 min, 75%.

All 21 new compounds were evaluated *in vitro*, first on the HepG2 cell line to determine their influence on cell viability (cytotoxic concentration 50% = CC_{50}), using doxorubicin as control. *In vitro* activity of these compounds was then measured on the promastigote form of *L. donovani* and on the trypomastigote blood stream form (BSF) of *T. b. brucei*. Their efficacy was compared to commercial reference drugs amphotericin B, miltefosine, fexinidazole, suramin, eflornithine and fexinidazole. The results obtained are presented in **Table 1**.

Table 1. *In vitro* bioevaluation of molecules **5-25** on *L. donovani* promastigotes, *T. b. brucei* BSF trypomastigotes and on the human HepG2 cell line.

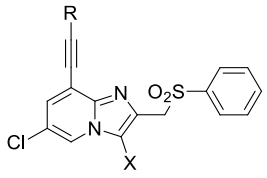

5 to **24**: X = NO_2
25: X = NH_2

Compd	R	Cell viability	Activity			
		CC_{50} HepG2 (µM)	EC_{50} *L. donovani* pro. (µM)	SI *Leishmania*	EC_{50} *T. b. brucei* BSF (µM)	SI *Trypanosoma*
5		>3.9[a]	-	-	-	-
6	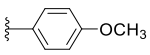	>3.9[a]	-	-	-	-
7	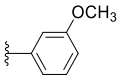	>3.9[a]	-	-	-	-
8		>3.9[a]	-	-	-	-
9		>3.9[a]	-	-	-	-
10		>3.9[a]	-	-	-	-
11		>3.9[a]	-	-	-	-
12	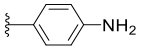	>3.9[a]	-	-	-	-
13		>3.9[a]	-	-	-	-
14		>3.9[a]	-	-	-	-
15	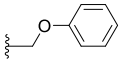	8.4 ± 2.3	1.3 ± 0.1	6.5	0.16 ± 0.03	52.5

16	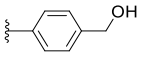	>15.6[a]	1.6 ± 0.1	>9.8	0.16 ± 0.03	>97.5
17	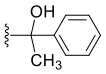	18.8 ± 2.2	1.0 ± 0.2	18.8	0.13 ± 0.04	>144.6
18		10.1 ± 1.4	3.9 ± 0.1	2.6	0.12 ± 0.03	84.2
19		>125[a]	7.4 ± 0.5	>16.9	0.07 ± 0.01	>1785.7
20		44.2 ± 11.2	4.7 ± 0.2	9.4	0.04 ± 0.01	1105
21		>62.5[a]	3.0 ± 0.4	>20.8	0.12 ± 0.03	>520.8
22	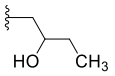	>62.5[a]	1.6 ± 0.7	>39.1	0.04 ± 0.008	>1562.5
23		>31.3[a]	1.7 ± 0.2	>18.4	0.10 ± 0.03	>313
24		>25[a]	1.0 ± 0.4	>25	0.10 ± 0.04	>250
25	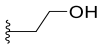	>62.5[a]	>62.5[a]	-	6.8 ± 1.05	>9.2
Ref. 1	Hit **A** molecule	>31[a]	1.8 ± 0.8	>17.2	2.9 ± 0.5	>10.7
Ref. 2	Hit **B** molecule	>50	1.2 ± 0.4	>41.7	0.25 ± 0.01	>200
Ref. 3	Hit **C** molecule	>100	1.0 ± 0.3	>100	1.3 ± 0.1	>76.9
Ref. 4	Doxorubicin[b]	0.2 ± 0.02	-	-	-	-
Ref. 5	Amphotericin B[d]	8.8 ± 0.3	0.07 ± 0.01	125.7	-	-
Ref. 6	Miltefosine[d]	85 ± 8.8	3.1 ± 0.2	27.4	-	-
Ref. 7	Fexinidazole[d,e]	>200[c]	1.2 ± 0.2	>166.7	0.6 ± 0.2	>333
Ref. 8	Suramin[e]	>100[c]	-	-	0.03 ± 0.009	>3333
Ref. 9	Eflornithine[e]	>100[c]	-	-	13.3 ± 2.1	>7.5
Ref. 10	Nifurtimox[e]	45.2 ± 1.3	-	-	2.6 ± 0.8	17.4

[a] The product could not be tested at higher concentrations due to a poor solubility in aqueous medium

[b] Doxorubicin was used as a cytotoxic reference drug

[c] The EC_{50} or CC_{50} value was not reached at the highest tested concentration

[d] Amphotericin B, Miltefosine and Fexinidazole were used as antileishmanial reference drugs

[e] Fexinidazole, Suramin, Eflornithine and Fexinidazole were used as anti-*Trypanosoma brucei* reference drugs

[f] SI = CC_{50} HepG2 / EC_{50} *L. infantum*

[g] SI = CC_{50} HepG2 / EC_{50} *T. brucei brucei*

Compounds **5-14**, which did not bear an alcohol function, could not be evaluated *in vitro* because of a lack of aqueous solubility. Most compounds in the series did not show a cytotoxic character in comparison with doxorubicin: four compounds (**15** to **18**) showed some decrease in cell viability with CC_{50} values below 20 µM whereas 6 molecules (**19** to **24**) displayed low values on the HepG2 cell line (>25 to >125 µM). Eleven molecules (**15-25**) were tested on *L. donovani* promastigotes: their EC_{50} ranged from 1 µM to 7.4 µM, values comparable to the previously identified hit molecules in the series. These activities are also very similar to those of fexinidazole and miltefosine, respectively 1.2 µM and 3.1 µM. Good CC_{50} values in this series, due to better water solubility of hydroxylated molecules, allowed to reach selectivity indices (SI) that are comparable or superior to that of miltefosine, as for example with the two best antileishmanial molecules in this series, compounds **22** and **24** (>39.1 and >25, respectively). All soluble compounds in the

experimental conditions (**15-24**) were evaluated on *T. b. brucei* BSF trypomastigotes. Quite interestingly, they all displayed significantly improved EC_{50} values ($40 \leq EC_{50} \leq 160$ nM) compared to previously identified hit molecules **A**, **B** and **C** ($25 \leq EC_{50} \leq 2900$ nM); these activity values were all better than the ones of fexinidazole (EC_{50} = 0.6 µM) and nifurtimox (EC_{50} = 2.6 µM). High selectivity indices were achieved with most of these derivatives, hit molecule **19** reaching the highest value (> 1786). This SI value appeared as quite significant when comparing to those of suramin (> 3333), fexinidazole (> 333), nifurtimox (17.4) and eflornithine (> 7.5) and hit **B** (best antitrypanosomal hit previously identified in the series with SI > 200). Derivatives with a tertiary alcohol function (**17**, **21**, **23**, **24**) tend to show reduced activities on *Trypanosoma brucei* BSF trypomastigotes than those bearing a secondary alcohol function (**20**, **22**). Likewise, molecules bearing a hydroxy group in *alpha* position of the alkyne function (**17**, **18**, **20**) tend to decrease cell viability on the HepG2 cell line more than those bearing a hydroxyl group in *beta* position of the triple bond (**19**, **22**). As expected, compared with nitrated molecule **19**, the amino-derivative **25** showed a 2 log decrease in antitrypanosomal activity (EC_{50} = 6,8 µM), pointing out the key role of the nitro group in the pharmacophore. Thus, because molecule **19** presented the best compromise between *in vitro* activity, water solubility, cytotoxicity and selectivity index, it was selected as the hit-compound of this novel series.

To deeper evaluate the antitrypanosomatid potential of **19**, its activity was measured against *L. infantum* axenic amastigotes and *T. cruzi* amastigotes, in addition to its cytotoxicity on the human macrophage THP1 cell line (**Table 2**). Thus, molecule **19** did not show a very promising antileishmanial profile (EC_{50} = 7.4 & 10.7 µM) whereas it displayed a good anti-*T. cruzi* activity (EC_{50} = 1.2 µM), similar to those of benznidazole and fexinidazole (0.5 and 3.0 µM, respectively).

Table 2. Summary of the *in vitro* antitrypanosomatid profile of hit compound **19**.

Compound	EC_{50} (µM)				CC_{50} (µM)	
	***L. donovani* promast.**	***L. inf.* axenic amast.**	***T. b. brucei* BSF**	***T. cruzi* amast.**	**HepG2**	**THP1**
19	7.4 ± 0.5	10.7 ± 0.7	0.07 ± 0.01	1.2 ± 0.8	>125[d]	>100[d]
Doxorubicin[a]	-	-	-	-	0.2 ± 0.02	0.7 ± 0.07
Miltefosine[b]	3.1 ± 0.2	0.8 ± 0.2	-	-	85 ± 8.8	35 ± 2.4
Fexinidazole[b,c]	1.2 ± 0.2	3.4 ± 0.8	0.6 ± 0.2	3.0 ± 0.1	>200[e]	>200[e]
Benznidazole[c]	-	-	1.8 ± 0.3	0.5 ± 0.1	>200[e]	>200[e]

[a] Doxorubicin was used as a cytotoxic reference drug
[b] Miltefosine and Fexinidazole were used as antileishmanial reference drugs
[c] Fexinidazole and Benznidazole were used as antitrypanosomal reference drugs
[d] The product could not be tested at higher concentrations in aqueous medium
[e] The CC_{50} or EC_{50} value was not reached at the highest tested concentration

In order to ensure that this novel series contained compounds that were substrates of parasitic NTRs (**Table 3**), hit molecules **19** and **22** were assayed against *L. donovani* promastigotes corresponding to the wild type, NTR1- and NTR2-overexpressing strains. Molecules **19** and **22** were twenty to forty times more effective against the strain overexpressing (OE) NTR1 than on the NTR2-overexpressing strain, indicating that these compounds are selectively bioactivated by *L. donovani* type 1 NTR. In the same way in *T. b. brucei*, it was also demonstrated that trypanosomal type 1 NTR was responsible for the bioactivation of **19** and **22**, these latter being 3 to 5 times more potent on the NTR-overexpressing strain than on the wild type. These results were consistent with those obtained with previous hit molecules, suggesting that introducing an alkynyl group at position 8 of the imidazo[1,2-*a*]pyridine pharmacophore preserves its bioactivation by type 1 NTRs.

Table 3. Sensitivity of wild-type and NTR-overexpressing *L. donovani* promastigotes and *T. brucei* BSF trypomastigotes strains to hit molecules **19** and **22**.

Compound	***L. donovani* promastigote EC_{50} (µM)**		
	Wild-type	**$NTR1^{OE}$**	**$NTR2^{OE}$**
19	21.4 ± 6	0.5 ± 0.05	24.5 ± 5.9
22	7.3 ± 0.6	0.4 ± 0.01	8.5 ± 0.3
***Hit A*[22]**	*1.9 ± 0.08*	*0.07 ± 0.002*	*3.0 ± 0.08*
***Hit B*[22]**	*1.5 ± 0.05*	*0.04 ± 0.009*	*2.0 ± 0.2*
***Hit C*[23]**	*0.26 ± 0.01*	*0.033 ± 0.007*	*0.3 ± 0.01*
Compound	***T. brucei* BSF trypomastigote EC_{50} (nM)**		
	Wild-type	**$NTR1^{OE}$**	
19	124.3 ± 7.2	26.5 ± 1.4	
22	200.0 ± 10.5	66.3 ± 4.8	
Nifurtimox	*1870 ± 0.05*	*600 ± 0.05*	

With regard to a mechanism of action involving an initial reductive bioactivation by NTRs, an electrochemistry study was carried out by measuring, in DMSO, the redox potentials of six 8-alkynylimidazo[1,2-*a*]pyridine derivatives, using cyclic voltammetry (**Figure 3**). The redox potentials values measured were corrected with respect to the normal hydrogen electrode (NHE). They correspond to a reversible one electron reduction/oxidation (redox couple = nitro group/anion radical counterpart).

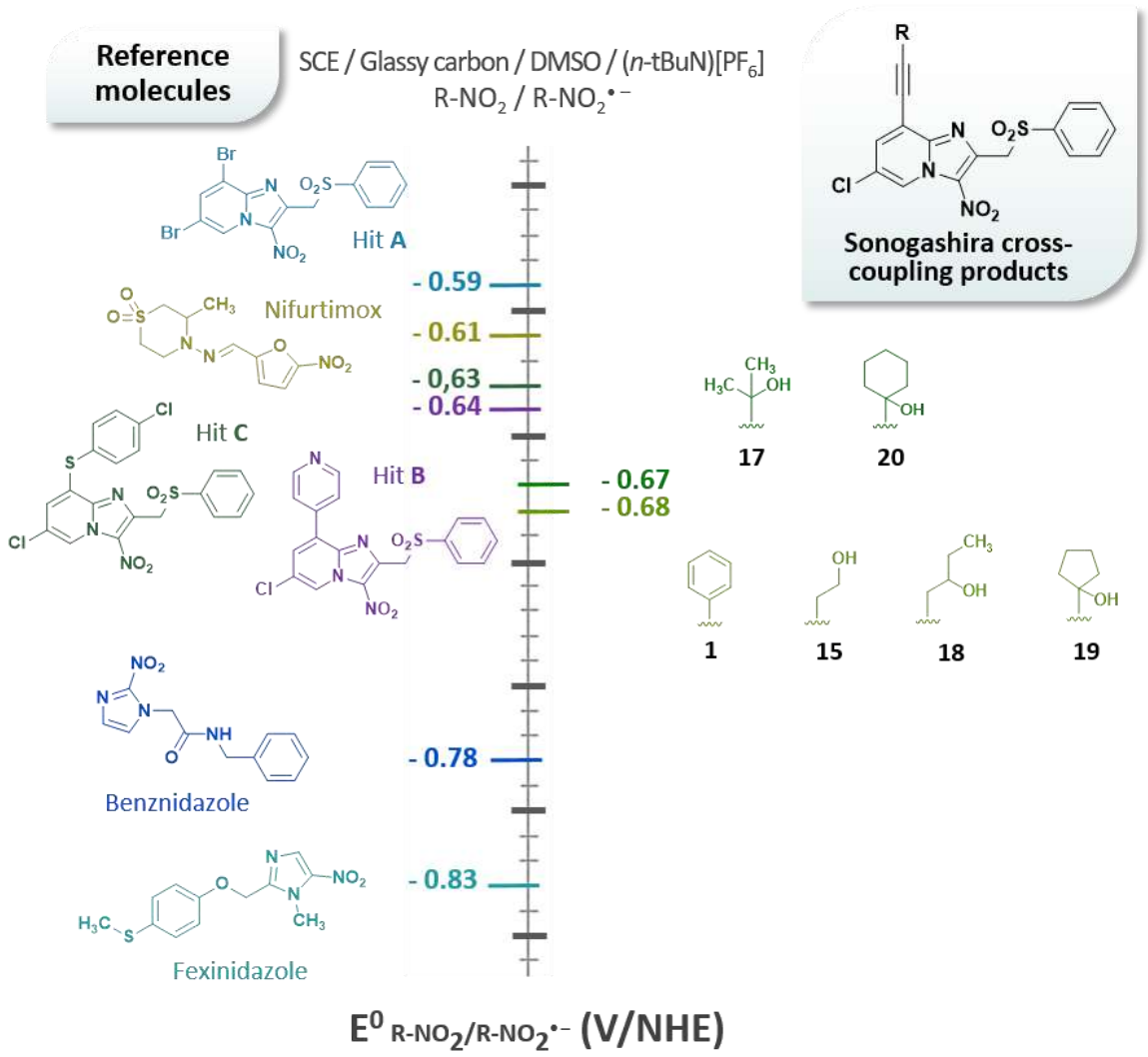

Figure 3: Redox potentials (E°) determined by cyclic voltammetry and given versus NHE. Conditions: selected compounds (10^{-3} mol.L^{-1}) in non-aqueous medium (DMSO + 0.1 mol.L^{-1} (*n*-Bu$_4$N)[PF$_6$]) on GC microdisk (r = 0.5 mm) at room temperature. Scan rate: 0.2 V.s^{-1}. Corriger N° des molécules

Redox potentials within this series appeared to be very homogeneous, with values of -0.67 V/NHE (**21**, **24**) and -0.68 V/NHE (**5**, **19**, **22**, **23**). The nature of the alkyne group at position 8 does not have an influence on the redox potential of the pharmacophore. However, in comparison with hit **A** (-0.59 V/NHE), hit **B** (-0.64 V/NHE) and hit **C** (-0.63 V/NHE), molecules with an alkynyl group at position 8 displayed lower redox potential values, ranging in between the ones of nifurtimox (-0.61 V/NHE) and fexinidazole (- 0.83 V/NHE).

The mutagenicity of many nitroaromatic molecules has always been a major concern, limiting the development of many of these derivatives. For fexinidazole, NTR-dependent mutagenic activity

was observed in Ames test, related to the expression of these enzymes by the *Salmonella typhimurium* strains used in this assay. However, evaluation of its genotoxicity by micronucleus test (*in vitro* on human cells and *in vivo* in rats) was negative [27]. Thus, a positive Ames test when evaluating nitroaromatic compounds has limited predictive values for humans, considering that there are no NTRs in mammalian cells and that most of nitroaromatics only display genotoxic properties after being bioactivated into reduced metabolites. Although the Ames test remains the most common method for assessing the mutagenicity of a substance, it is nowadays accepted that the comet assay or the micronucleus assay, using mammalian cells, are better *in vitro* alternatives for evaluating the potential genotoxicity of nitroheterocyclic molecules. Considering molecule **19**, an Ames test in metabolizing conditions and a comet assay were performed simultaneously and showed that, despite presenting mutagenic properties (Ames test) at 0.25 or 2.5 mM, compound **19** was not genotoxic in the comet assay after a 2 or 72 h exposure, at 20 or 30 µM. These results are consistent with those obtained with fexinidazole and with previously identified hit molecules in 3-nitroimidazo[1,2-*a*]pyridine series, representing an great improvement over nifurtimox and benznidazole which are known to be genotoxic over mammalian cells [9].

Then, some *in vitro* physicochemical and pharmacokinetic parameters of hit compound **19** were determined (**Table 4**): **19** is a lipophilic molecule (cLogP = 2.5) that shows good aqueous solubility (thermodynamic solubility = 71 µM), due to its hydroxyl group, that strongly binds to human albumin (98.5%) and whose microsomal stability was significantly improved ($T_{1/2}$ = 16 min), in comparison with previously identified hit-compounds in the series ($T_{1/2}$ = 3 to 9 min). Hit compound **19** was also shown to cross the blood brain barrier according to a PAMPA BBB assay, in accordance with its high CNS MPO score (4.35) [28].

Table 4. Physicochemical, pharmacokinetic and toxicological data regarding hit compound **19**

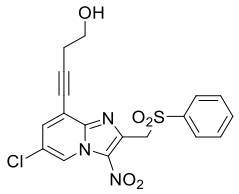

Compound **19**

cLogP[a]	2.49
Thermodynamic solubility (µM)	70.7 ± 2.8
Binding to human albumin (%)	98.5
Microsomal stability: $T_{1/2}$ (min)	16
PAMPA Blood-brain barrier permeability assay : P_e (nm/s)	346.1 ± 89.2
CNS MPO score	4.35
C_{max} in mouse (ng/mL)	393.96 ± 156.36
T_{max} in mouse (h)	0.83 ± 0.29
Plasma half-life in mouse (h)	10.01 ± 3.02
$AUC_{0\text{-}inf}$ (ng.h/mL)	1433.05 ± 69.92
Clearance (mL/h)	2.44 ± 0.03
Ames test (0.25 and 2.5 mM + S9mix on 4 strains)	Positive
Comet assay (after 2 and 72 h & 20 and 30 µM)	Negative

[a] Weighted clogP was computed by Marvin® (ChemAxon)

Finally, compound **19** was administered orally to mice to determine its maximal tolerated dose and its main *in vivo* pharmacokinetic parameters**.** A once daily repeated oral administration (intragastrical gavage) of **19** at 100 mg/kg for 5 days was well tolerated in mice. Thus, the No Observed Adverse Event Level (NOAEL) in mice was set at 100 mg/kg/day. After euthanasia, no lesions were found on the different organs (kidney, liver, brain, heart and lung). Pharmacokinetics parameters were determined to understand the behavior of **19** after oral administration. The main pharmacokinetics parameters are shown in **Table 4**. Hit compound **19** is orally absorbed and shows a long plasma half-life (10 h), parameters that are encouraging for further development.

3. Conclusion

Pharmacomodulation at position 8 of the imidazo[1,2-*a*]pyridine scaffold, using the Sonogashira cross-coupling reaction, led to 20 original alkynyl derivatives. These displayed modest *in vitro* antileishmanial activity, whereas several hydroxylated derivatives showed very good *in vitro* activities on *T. b. brucei* bloodstream forms and low cytotoxicities against a human hepatocyte cell line (7 molecules with SI > 100 and 2 molecules with SI > 1000). The lead compound of this series (**19**) was also tested *in vitro* on *T. cruzi* and showed good EC_{50} values, two times lower than that of fexinidazole. Its mechanism of action involves activation by the parasite NTR1. Moreover, nitroaromatic hit-molecule **19** was not genotoxic in the comet assay which represents a significant improvement over nifurtimox and benznidazole. Study of *in vitro* physicochemical and pharmacokinetic parameters of molecule **19** showed improved properties in the imidazo[1,2-*a*]pyridine series, regarding in particular water solubility and microsomal stability. In the mouse, **19** was orally absorbed and well tolerated after repeated administrations of 100 mg/kg for 5 days. Its plasma half-life (10 h) is encouraging and allows further determination of its activity in an infected mouse model, to try to identify a novel antitrypanosomal lead compound.

4. Experimental section

4.1. Chemistry

4.1.1. Synthesis

Commercial reagents were used as received without additional purification. Melting points were determined in open capillary tubes with a Büchi apparatus and are uncorrected. Elemental analysis and HRMS were carried out at the Spectropole, Faculté des Sciences et Techniques de Saint-Jérôme, Marseille, France. NMR spectra were recorded on a Bruker ARX 200 spectrometer or a Bruker AV 250 spectrometer at the Faculté de Pharmacie de Marseille, or a BRUKER Avance III nanobay 400 spectrometer at the the Spectropole, Faculté des Sciences et Techniques de Saint-Jérôme, Marseille, or on a Bruker UltraShield 300 MHz or a Bruker IconNMR 400 MHz spectrometer at the Laboratoire de Chimie de Coordination, Toulouse (^{1}H-NMR: 200, 250, 300 or 400 MHz, ^{13}C-NMR: 50, 63, 75 or 100 MHz). NMR references were the following: ^{1}H: $CHCl_3$ δ = 7.26, DMSO-d_6 δ = 2.50, Acetone-d_6 δ = 2.05 and ^{13}C: $CHCl_3$ δ = 76.9, DMSO-d_6 δ = 39.5,

Acetone-d_6 δ = 29.9. Solvents were dried by conventional methods. The following adsorbent was used for column chromatography: silica gel 60 (Merck, particle size 0.063–0.200 mm, 70–230 mesh ASTM). TLC was performed on 5 cm × 10 cm aluminium plates coated with silica gel 60F-254 (Merck) in an appropriate eluent. Visualization was made with ultraviolet light (254 nm). HRMS spectra were recorded on QStar Elite (Applied Biosystems SCIEX) spectrometer. PEG was the matrix for HRMS. The experimental exact mass was given for the ion which has the maximum isotopic abundance. Purity of synthetized compounds was checked with LC-MS analyses which were realized at the Faculté de Pharmacie de Marseille with a Thermo Scientific Accela High Speed LC System® coupled with a single quadrupole mass spectrometer Thermo MSQ Plus®. The RP-HPLC column used is a Thermo Hypersil Gold® 50 × 2.1 mm (C18 bounded), with particles of 1.9 µm diameter. The volume of sample injected on the column was 1 µL. The chromatographic analysis, total duration of 8 min, is made with the gradient of following solvents: t = 0 min, water/methanol 50/50; 0 < t < 4 min, linear increase in the proportion of methanol to a ratio water/methanol 5/95; 4 < t < 6 min, water/methanol 5/95; 6 < t < 7 min, linear decrease in the proportion of methanol to return to a ratio 50/50 water/methanol; 6 < t < 7 min, water/methanol 50/50. The water used was buffered with 5 mM ammonium acetate. The retention times (t_R) of the molecules analyzed are indicated in min.

Molecules **1**-**4** were previously described [22].

4.1.1.1. General procedure for the preparation of 8-alkynylimidazo[1,2-*a*]pyridine derivatives (5 to 24)

A mixture of 8-bromo-6-chloro-3-nitro-2-(phenylsulfonylmethyl)imidazo[1,2-*a*]pyridine **4** (400 mg, 1 equiv.), tetrakis(triphenylphosphine)palladium(0) (107.3 mg, 0.1 equiv.), copper iodide (17.7 mg, 0.1 equiv.), diisopropylamine (1.57 mL, 12 equiv.), appropriate alkyne (1.5 equiv.), in THF (15 mL) was stirred under N_2 at room temperature until complete disappearance of the starting material (as monitored by LC/MS or TLC). Water was then added and the mixture was extracted three times with dichloromethane. The organic layer was washed three times with water, dried over $MgSO_4$, filtered and evaporated. The crude residue was purified by column chromatography on silica gel (with appropriate eluent) and recrystallized from the appropriate solvent, affording compounds **1** to **20**.

4.1.1.2. 6-Chloro-3-nitro-8-(phenylethynyl)-2-(phenylsulfonylmethyl)imidazo[1,2-*a*]pyridine (5)

Compound **5** was obtained after purification by chromatography (eluent: dichloromethane/cyclohexane/diethyl ether 6.9/3/0.1) and recrystallization from acetonitrile as a yellow solid in 90% yield (0.38 g). mp 228 °C. ^{1}H NMR (400 MHz, $CDCl_3$) δ: 5.19 (2H, s), 7.40–

7.47 (3H, m), 7.50–7.54 (2H, m), 7.59–7.63 (3H, m), 7.79 (1H, d, *J* = 1.9 Hz), 7.88–7.91 (2H, m), 9.41 (1H, d, *J* = 1.9 Hz). ^{13}C NMR (100 MHz, $CDCl_3$) *δ*: 56.9 (CH_2), 81.5 (C), 99.8 (C), 115.7 (C), 121.6 (C), 124.9 (CH), 125.5 (C), 128.7 (2 CH), 128.8 (2 CH), 129.3 (2 CH), 130.0 (CH), 131.3 (C), 132.4 (2 CH), 134.2 (CH), 134.5 (CH), 139.3 (C), 139.8 (C), 143.0 (C). LC/MS ESI$^+$ t_R 3.99 min, (m/z) $[M+H]^+$ 451.83/453.84. HRMS (+ESI): 452.0462 $[M+H]^+$. Calcd for $C_{22}H_{14}ClN_3O_4S$: 452.0466.

4.1.1.3. 6-Chloro-8-(4-methoxyphenylethynyl)-3-nitro-2-(phenylsulfonylmethyl)imidazo[1,2-*a*]pyridine (6)

Compound **6** was obtained after purification by chromatography (eluent: dichloromethane/cyclohexane 9/1) and recrystallization from acetonitrile as a yellow solid in 51% yield (0.29 g). mp 210 °C. ^{1}H NMR (400 MHz, $CDCl_3$) *δ*: 3.88 (3H, s), 5.19 (2H, s), 6.92–6.94 (2H, m), 7.50–7.55 (4H, m), 7.60–7.64 (1H, m), 7.74 (1H, d, *J* = 1.9 Hz), 7.88–7.91 (2H, m), 9.37 (1H, d, *J* = 1.9 Hz). ^{13}C NMR (100 MHz, $CDCl_3$) *δ*: 55.6 (CH_3), 56.9 (CH_2), 80.7 (C), 100.4 (C), 113.6 (C), 114.3 (2 CH), 116.1 (C), 124.5 (CH), 125.5 (C), 128.8 (2 CH), 129.3 (2 CH), 131.3 (C), 134.0 (CH), 134.1 (2 CH), 134.2 (CH), 139.3 (C), 139.8 (C), 143.0 (C), 161.0 (C). LC/MS ESI$^+$ t_R 4.09 min, (m/z) $[M+H]^+$ 480.61/483.87. HRMS (+ESI): 482.0569 (M + H^+). Calcd for $C_{23}H_{16}ClN_3O_5S$: 482.0572.

4.1.1.4. 6-Chloro-8-(3-methoxyphenylethynyl)-3-nitro-2-(phenylsulfonylmethyl)imidazo[1,2-*a*]pyridine (7)

Compound **7** was obtained after purification by chromatography (eluent: chloroform/diethyl ether 9.9/0.1) as a yellow solid in 47% yield (0.21 g). mp 171 °C. ^{1}H NMR (400 MHz, Acetone-d_6) *δ*: 3.89 (3H, s), 5.22 (2H, s), 7.08–7.12 (2H, m), 7.17–7.19 (1H, m), 7.40–7.44 (1H, m), 7.58–7.62 (2H, m), 7.69–7.73 (1H, m), 7.84–7.86 (2H, m), 8.04 (1H, d, *J* = 1.9 Hz), 9.42 (1H, d, *J* = 1.9 Hz). ^{13}C NMR (100 MHz, Acetone-d_6) *δ*: 54.9 (CH_3), 56.1 (CH_2), 81.5 (C), 97.9 (C), 114.5 (C), 116.1 (CH), 116.6 (CH), 122.6 (C), 124.1 (C), 124.2 (CH), 125.6 (CH), 128.5 (2 CH), 129.0 (2 CH), 129.84 (CH), 131.5 (C), 133.9 (CH), 134.1 (CH), 139.5 (C), 139.7 (C), 142.7 (C), 159.7 (C). LC/MS ESI$^+$ t_R 4.09 min, (m/z) $[M+H]^+$ 480.70/483.65. HRMS (+ESI): 482.0569 (M + H^+). Calcd for $C_{23}H_{16}ClN_3O_5S$: 482.0572.

4.1.1.5. 6-Chloro-8-(2-methoxyphenylethynyl)-3-nitro-2-(phenylsulfonylmethyl)imidazo[1,2-*a*]pyridine (8)

Compound **8** was obtained after purification by chromatography (eluent: dichloromethane/cyclohexane/diethyl ether 6.9/3/0.1) and recrystallization from acetonitrile as a yellow solid in 67% yield (0.30 g). mp 204 °C. ^{1}H NMR (400 MHz, $CDCl_3$) *δ*: 3.96 (3H, s), 5.19

(2H, s), 6.94–7.01 (2H, m), 7.39–7.44 (1H, m), 7.49–7.54 (3H, m), 7.58–7.62 (1H, m), 7.80 (1H, d, *J* = 1.9 Hz), 7.89–7.91 (2H, m), 9.38 (1H, d, *J* = 1.9 Hz). ^{13}C NMR (100 MHz, DMSO-d_6) δ: 56.3 (CH_3), 56.4 (CH_2), 86.0 (C), 95.4 (C), 110.4 (C), 112.1 (CH), 114.4 (C), 121.1 (CH), 124.2 (C), 126.3 (CH), 128.7 (2 CH), 129.7 (2 CH), 131.7 (C), 132.2 (CH), 134.0 (CH), 134.6 (CH), 134.9 (CH), 139.2 (C), 139.8 (C), 142.9 (C), 160.5 (C). LC/MS ESI$^+$ t_R 3.86 min, (m/z) [M+H]$^+$ 480.62/483.88. HRMS (+ESI): 482.0570 (M + H$^+$). Calcd for $C_{23}H_{16}ClN_3O_5S$: 482.0572.

4.1.1.6. 6-Chloro-8-(4-fluorophenylethynyl)-3-nitro-2-(phenylsulfonylmethyl)imidazo[1,2-*a*]pyridine (9)

Compound **9** was obtained after purification by chromatography (eluent: dichloromethane/cyclohexane 7/3) and recrystallization from acetonitrile as a yellow solid in 49% yield (0.21 g). mp 245 °C. ^{1}H NMR (250 MHz, DMSO-d_6) δ: 5.31 (2H, s), 7.36–7.43 (2H, m), 7.57–7.67 (4H, m), 7.70–7.73 (1H, m), 7.76–7.81 (2H, m), 8.26 (1H, s), 9.35 (1H, s). ^{13}C NMR (100 MHz, DMF-d_7) δ: 56.7 (CH_2), 82.3 (C), 97.1 (C), 114.4 (C), 116.7 (2 CH, d, *J* = 22.6 Hz), 118.3 (C, d, *J* = 3.3 Hz), 124.5 (C), 126.5 (CH), 128.9 (2 CH), 129.7 (2 CH), 132.1 (C), 134.6 (CH), 134.8 (2 CH, d, *J* = 8.9 Hz), 135.0 (CH), 139.8 (C), 140.1 (C), 143.2 (C), 164.9 (C). LC/MS ESI$^+$ t_R 4.01 min, (m/z) [M+H]$^+$ 469.70/471.23. HRMS (+ESI): 470.0371 (M + H$^+$). Calcd for $C_{22}H_{13}ClFN_3O_4S$: 470.0372.

4.1.1.7. 6-Chloro-8-(3-fluorophenylethynyl)-3-nitro-2-(phenylsulfonylmethyl)imidazo[1,2-*a*]pyridine (10)

Compound **10** was obtained after purification by chromatography (eluent: dichloromethane/cyclohexane/diethyl ether 6.8/3/0.2) and recrystallization from acetonitrile as a yellow solid in 38% yield (0.17 g). mp 240 °C. ^{1}H NMR (400 MHz, $CDCl_3$) δ: 5.19 (2H, s), 7.16–7.18 (1H, m), 7.28–7.65 (6H, m), 7.79 (1H, s), 7.89 (2H, d, *J* = 7.6 Hz), 9.42 (1H, s). ^{13}C NMR (100 MHz, $CDCl_3$) δ: 56.8 (CH_2), 82.2 (C), 98.1 (C), 115.2 (C), 117.4 (CH, d, *J* = 21.2 Hz), 119.1 (CH, d, *J* = 23 Hz), 123.3 (C, d, *J* = 9.43 Hz), 125.3 (CH), 125.4 (C), 128.2 (CH, d, *J* = 3.23 Hz), 128.2 (2 CH), 129.3 (2 CH), 130.3 (CH, d, *J* = 8.54 Hz), 131.3 (C), 134.3 (CH), 134.6 (CH), 139.3 (C), 139.9 (C), 142.9 (C), 162.5 (C, d, *J* = 247.6 Hz). LC/MS ESI$^+$ t_R 4.03 min, (m/z) [M+H]$^+$ 469.85/471.98. HRMS (+ESI): 470.0372 (M + H$^+$). Calcd for $C_{22}H_{13}ClFN_3O_4S$: 470.0372.

4.1.1.8. 6-Chloro-8-(2-fluorophenylethynyl)-3-nitro-2-(phenylsulfonylmethyl)imidazo[1,2-*a*]pyridine (11)

Compound **11** was obtained after purification by chromatography (eluent: dichloromethane/cyclohexane 8/2) and recrystallization from acetonitrile as a yellow solid in 65% yield (0.28 g). mp 229 °C. ^{1}H NMR (400 MHz, DMSO-d_6) δ: 5.30 (2H, s), 7.35–7.45 (2H, m),

7.56–7.72 (5H, m), 7.80 (2H, d, *J* = 7.1 Hz), 8.28 (1H, d, *J* = 1.9 Hz), 9.36 (1H, d, *J* = 1.9 Hz). ^{13}C NMR (100 MHz, DMSO-d_6) δ: 55.8 (CH_2), 86.7 (C), 90.7 (C), 109.4 (C, d, *J* = 15.4 Hz), 112.9 (C), 116.0 (CH, d, *J* = 20.2 Hz), 123.6 (C), 125.1 (CH, d, *J* = 3.58 Hz), 126.4 (CH), 128.2 (2 CH), 129.2 (2 CH), 131.3 (C), 132.5 (CH, d, *J* = 8.26 Hz), 133.8 (CH), 134.1 (CH), 135.1 (CH), 138.7 (C), 139.4 (C), 142.3 (C), 161.9 (C, d, *J* = 251.5 Hz). LC/MS ESI$^+$ t_R 3.95 min, (m/z) $[M+H]^+$ 469.83/471.49. HRMS (+ESI): 470.0371 ($M + H^+$). Calcd for $C_{22}H_{13}ClFN_3O_4S$: 470.0372.

4.1.1.9. 4-[6-Chloro-3-nitro-2-(phenylsulfonylmethyl)imidazo[1,2-*a*]pyridin-8-yl]ethynylaniline (12)

After washing the crude residue with acetone and filtration, compound **12** was obtained as an orange solid in 72% yield (0.31 g). mp 255 °C. ^{1}H NMR (400 MHz, DMSO-d_6) δ: 5.29 (2H, s), 5.90 (2H, s), 6.63 (2H, s), 7.22 (2H, s), 7.60–7.81 (5H, m), 8.06 (1H, s), 9.24 (1H, s). ^{13}C NMR (100 MHz, DMSO-d_6) δ: 55.8 (CH_2), 80.2 (C), 101.1 (C), 106.2 (C), 113.6 (2 CH), 114.8 (C), 123.8 (C), 124.6 (CH), 128.2 (2 CH), 129.2 (2 CH), 131.2 (C), 133.1 (CH), 133.2 (2 CH), 134.1 (CH), 138.7 (C), 139.2 (C), 142.4 (C), 150.8 (C). LC/MS ESI$^+$ t_R 3.28 min, (m/z) $[M+H]^+$ 466.80/468.68. HRMS (+ESI): 467.0572 ($M + H^+$). Calcd for $C_{22}H_{15}ClN_4O_4S$: 467.0575.

4.1.1.10. 6-Chloro-3-nitro-2-(phenylsulfonylmethyl)-8-(thiophen-2-ylethynyl)imidazo[1,2-*a*]pyridine (13)

Compound **13** was obtained after purification by chromatography (eluent: dichloromethane/cyclohexane/diethyl ether 5/4.5/0.5) and recrystallization from acetonitrile as a yellow solid in 65% yield (0.28 g). mp 220 °C. ^{1}H NMR (400 MHz, $CDCl_3$) δ: 5.19 (2H, s), 7.08–7.11 (1H, m), 7.44–7.66 (5H, m), 7.77 (1H, s), 7.89 (2H, d, *J* = 7.7 Hz), 9.40 (1H, s). ^{13}C NMR (100 MHz, $CDCl_3$) δ: 56.8 (CH_2), 85.3 (C), 93.2 (C), 115.4 (C), 121.4 (C), 124.9 (CH), 125.5 (C), 127.6 (CH), 128.8 (2 CH), 129.3 (2 CH), 129.8 (CH), 131.3 (C), 134.2 (CH), 134.3 (CH), 134.5 (CH), 139.2 (C), 139.8 (C), 142.6 (C). LC/MS ESI$^+$ t_R 3.79 min, (m/z) $[M+H]^+$ 457.72/459.88. HRMS (+ESI): 458.0031 ($M + H^+$). Calcd for $C_{20}H_{12}ClN_3O_4S_2$: 458.0031.

4.1.1.11. 6-Chloro-3-nitro-2-(phenylsulfonylmethyl)-8-(pyridin-3-ylethynyl)imidazo[1,2-*a*]pyridine (14)

Compound **14** was obtained after purification by chromatography (eluent: chloroform/diethyl ether 8/2) as a yellow solid in 36% yield (0.15 g). mp 240 °C. ^{1}H NMR (400 MHz, DMSO-d_6) δ: 5.31 (2H, s), 7.56–7.61 (3H, s), 7.68–7.72 (1H, s), 7.79–7.81 (2H, m), 7.99–8.02 (1H, m), 8.30 (1H, d, *J* = 1.9 Hz), 8.70 (1H, dd, *J* = 1.6 Hz and 4.9 Hz), 8.77 (1H, d, *J* = 1.6 Hz), 9.37 (1H, d, *J* = 1.9 Hz). ^{13}C NMR (100 MHz, DMSO-d_6) δ: 55.8 (CH_2), 85.0 (C), 94.2 (C), 112.8 (C), 118.2 (C), 123.6 (C), 123.9 (CH), 126.5 (CH), 128.3 (2 CH), 129.2 (2 CH), 131.3 (C), 134.1 (CH), 135.1

(CH), 138.7 (C), 138.9 (CH), 139.4 (C), 142.2 (C), 150.1 (CH), 151.8 (CH). LC/MS ESI$^+$ t_R 2.91 min, (m/z) $[M+H]^+$ 452.77/454.84. HRMS (+ESI): 453.0417 (M + H^+). Calcd for $C_{21}H_{13}ClN_4O_4S$: 453.0419.

4.1.1.12. 6-Chloro-3-nitro-8-(3-phenoxyprop-1-yn-1-yl)-2-(phenylsulfonylmethyl)imidazo[1,2-*a*]pyridine (15)

Compound **15** was obtained after purification by chromatography (eluent: dichloromethane/ethyl acetate 9.8/0.2) as a dark solid in 74% yield (0.33 g). mp 72 °C. ^{1}H NMR (250 MHz, DMSO-d_6) δ: 5.17 (2H, s), 5.27 (2H, s), 6.98–7.09 (2H, m), 7.32–7.39 (3H, m), 7.56–7.62 (2H, m), 7.70–7.80 (3H, m), 8.16 (1H, d, J = 1.7 Hz), 9.31 (1H, d, J = 1.9 Hz). ^{13}C NMR (62.5 MHz, DMSO-d_6) δ: 55.8 (CH_2), 56.0 (CH_2), 79.0 (C), 93.8 (C), 112.6 (C), 114.9 (2 CH), 121.4 (CH), 123.5 (C), 126.3 (CH), 128.1 (2 CH), 129.2 (2 CH), 129.5 (2 CH), 131.2 (C), 134.1 (CH), 135.2 (CH), 138.7 (C), 139.2 (C), 142.5 (C), 157.3 (C). LC/MS ESI$^+$ t_R 3.73 min, (m/z) $[M+H]^+$ 480.60/483.76. HRMS (+ESI): 482.0572 (M + H^+). Calcd for $C_{23}H_{16}ClN_3O_5S$: 482.0572.

4.1.1.13. 6-Chloro-8-[(4-hydroxymethyl)phenylethynyl]-3-nitro-2-(phenylsulfonylmethyl)imidazo[1,2-*a*]pyridine (16)

Compound **16** was obtained after purification by chromatography (eluent: dichloromethane/ethyl acetate 9/1) and recrystallization from propan-2-ol as a pale yellow solid in 68% yield (0.30 g). mp 187 °C. ^{1}H NMR (250 MHz, DMSO-d_6) δ: 4.58 (2H, d, J = 5.4 Hz), 5.31 (2H, s), 5.38 (1H, t, J = 5.6 Hz), 7.44–7.48 (2H, m), 7.52–7.63 (4H, m), 7.70–7.75 (1H, m), 7.79–7.82 (2H, m), 8.24 (1H, d, J = 1.7 Hz), 9.33 (1H, d, J = 1.8 Hz). ^{13}C NMR (62.5 MHz, DMSO-d_6) δ: 55.8 (CH_2), 62.4 (CH_2), 81.7 (C), 98.0 (C), 113.6 (C), 119.0 (C), 123.6 (C), 125.8 (CH), 126.7 (2 CH), 128.2 (2 CH), 129.2 (2 CH), 131.2 (C), 131.5 (2 CH), 134.1 (CH), 134.5 (CH), 138.7 (C), 139.3 (C), 142.3 (C), 144.8 (C). LC/MS ESI$^+$ t_R 3.29 min, (m/z) $[M+H]^+$ 480.61/483.75. HRMS (+ESI): 482.0571 (M + H^+). Calcd for $C_{23}H_{16}ClN_3O_5S$: 482.0572.

4.1.1.14. 4-[6-Chloro-3-nitro-2-(phenylsulfonylmethyl]imidazo[1,2-*a*]pyridin-8-yl)-2-phenylbut-3-yn-2-ol (17)

Compound **17** was obtained after purification by chromatography (eluent: dichloromethane/methanol 9.8/0.2) and recrystallization from propan-2-ol as a yellow solid in 72% yield (0.33 g). mp 160 °C. ^{1}H NMR (250 MHz, DMSO-d_6) δ: 1.77 (3H, s), 5.30 (2H, s), 6.48 (1H, s), 7.31–7.46 (3H, m), 7.56–7.62 (2H, m), 7.70–7.75 (3H, m), 7.81–7.84 (2H, m), 8.18 (1H, s), 9.35 (1H, s). ^{13}C NMR (62.5 MHz, DMSO-d_6) δ: 33.5 (CH_3), 56.0 (CH_2), 68.7 (C), 76.0 (C), 103.4 (C), 113.5 (C), 123.6 (C), 125.0 (2 CH), 125.8 (CH), 127.2 (CH), 128.0 (2 CH), 128.1 (2 CH), 129.2 (2 CH), 131.2 (C), 134.1 (CH), 134.7 (CH), 138.8 (C), 139.3 (C), 142.5 (C), 145.8 (C).

LC/MS ESI$^+$ t_R 3.66 min, (m/z) $[M+NH_4]^+$ 511.53/512.76/514.32. HRMS (+ESI): 518.0547 (M + Na^+). Calcd for $C_{24}H_{18}ClN_3O_5S$, Na^+: 518.0548.

4.1.1.15. 3-[6-Chloro-3-nitro-2-(phenylsulfonylmethyl)imidazo[1,2-*a*]pyridin-8-yl]prop-2-yn-1-ol (18)

Compound **18** was obtained after purification by chromatography (eluent: dichloromethane/ethyl acetate 9/1) as a white solid in 60% yield (0.23 g). mp 225 °C. ^{1}H NMR (300 MHz, DMSO-d_6) δ: 4.42 (2H, d, J = 5.54 Hz), 5.56 (2H, s), 5.58 (1H, t, J = 6.2 Hz), 7.58–7.63 (2H, m), 7.74–7.80 (3H, m), 8.11 (1H, s), 9.30 (1H, s). ^{13}C NMR (75 MHz, DMSO-d_6) δ: 49.6 (CH_2), 55.9 (CH_2), 76.4 (C), 99.0 (C), 113.5 (C), 123.6 (C), 125.9 (CH), 128.1 (2 CH), 129.3 (2 CH), 131.2 (C), 134.2 (CH), 134.8 (CH), 138.7 (C), 139.1 (C), 142.6 (C). LC/MS ESI$^+$ t_R 1.79 min, (m/z) $[M+NH_4]^+$ 422.88/425.02. HRMS (+ESI): 406.0259 (M + H^+). Calcd for $C_{17}H_{12}ClN_3O_5S$: 406.0259.

4.1.1.16. 4-[6-Chloro-3-nitro-2-(phenylsulfonylmethyl)imidazo[1,2-*a*]pyridin-8-yl]but-3-yn-1-ol (19)

Compound **19** was obtained after purification by chromatography (eluent: dichloromethane/methanol 9.5/0.5) and recrystallization from acetonitrile as a beige solid in 67% yield (0.26 g). mp 185 °C. ^{1}H NMR (400 MHz, $CDCl_3$) δ: 2.78–2.86 (3H, m), 3.89 (2H, s), 5.15 (2H, s), 7.55–7.67 (4H, m), 7.87–7.90 (2H, m), 9.37 (1H, s). ^{13}C NMR (100 MHz, $CDCl_3$) δ: 24.6 (CH_2), 56.8 (CH_2), 60.7 (CH_2), 75.1 (C), 100.1 (C), 115.8 (C), 124.7 (CH), 125.6 (C), 128.6 (2 CH), 129.4 (2 CH), 131.3 (C), 134.1 (CH), 134.3 (CH), 139.3 (C), 139.4 (C), 143.6 (C). LC/MS ESI$^+$ t_R 2.13 min, (m/z) $[M+H]^+$ 419.81/421.93. HRMS (+ESI): 420.0416 (M + H^+). Calcd for $C_{18}H_{14}ClN_3O_5S$: 420.0415.

4.1.1.17. 4-[6-Chloro-3-nitro-2-(phenylsulfonylmethyl)imidazo[1,2-*a*]pyridin-8-yl]but-3-yn-2-ol (20)

Compound **20** was obtained after purification by chromatography (eluent: dichloromethane/methanol 9.8/0.2) and recrystallization from propan-2-ol as a beige solid in 67% yield (0.26 g). mp 196 °C. ^{1}H NMR (300 MHz, $CDCl_3$) δ: 1.60 (3H, d, J = 6.1 Hz), 3.62 (1H, s), 4.88 (1H, bs), 5.18 (2H, s), 7.51–7.56 (2H, m), 7.64–7.70 (2H, m), 7.85–7.87 (2H, m), 9.36 (1H, s). ^{13}C NMR (75 MHz, $CDCl_3$) δ: 23.6 (CH_3), 56.6 (CH_2), 58.5 (CH), 75.9 (C), 102.3 (C), 114.8 (C), 125.0 (CH), 125.3 (C), 128.4 (2 CH), 129.3 (2 CH), 131.1 (C), 134.2 (CH), 134.7 (CH), 139.0 (C), 139.4 (C), 142.9 (C). LC/MS ESI$^+$ t_R 2.28 min, (m/z) $[M+NH_4]^+$ 436.88/438.9. HRMS (+ESI): 420.0418 (M + H^+). Calcd for $C_{18}H_{14}ClN_3O_5S$: 420.0415.

4.1.1.18. 4-[6-chloro-3-nitro-2-(phenylsulfonylmethyl)imidazo[1,2-*a*]pyridin-8-yl]-2-methylbut-3-yn-2-ol (21)

Compound **21** was obtained after purification by chromatography (eluent: dichloromethane/ethyl acetate 9/1) and recrystallization from propan-2-ol as a pale yellow solid in 78% yield (0.31 g). mp 193 °C. ^{1}H NMR (400 MHz, DMSO-d_6) δ: 1.50 (6H, s), 5.27 (2H, s), 5.71 (1H, s), 7.58–7.64 (2H, m), 7.72–7.81 (3H, m), 8.04 (1H, s), 9.30 (1H, s). ^{13}C NMR (100 MHz, DMSO-d_6) δ: 31.2 (2 CH_3), 55.9 (CH_2), 63.8 (C), 73.5 (C), 105.0 (C), 113.8 (C), 123.6 (C), 125.6 (CH), 128.1 (2 CH), 129.2 (2 CH), 131.2 (C), 134.2 (CH), 134.8 (CH), 138.8 (C), 139.2 (C), 142.4 (C). LC/MS ESI$^+$ t_R 2.73 min, (m/z) $[M+NH_4]^+$ 450.37/452.80. HRMS (+ESI): 434.0571 (M + H^+). Calcd for $C_{19}H_{16}ClN_3O_5S$: 434.0572.

4.1.1.19. 6-[6-Chloro-3-nitro-2-(phenylsulfonylmethyl)imidazo[1,2-*a*]pyridin-8-yl]hex-5-yn-3-ol (22)

Compound **22** was obtained after purification by chromatography (eluent: cyclohexane/ethyl acetate 4/5) and recrystallization from propan-2-ol as a white solid in 60% yield (0.25 g). mp 154 °C. ^{1}H NMR (400 MHz, DMSO-d_6) δ: 0.93 (3H, t, J = 7.4 Hz), 1.39–1.70 (2H, m), 2.63 (2H, d, J = 5.9 Hz), 3.59–3.69 (1H, m), 4.91 (1H, d, J = 5.2 Hz), 5.25 (2H, s), 7.58–7.63 (2H, m), 7.73–7.79 (3H, m), 8.04 (1H, d, J = 1.9 Hz), 9.28 (1H, d, J = 1.9 Hz). ^{13}C NMR (100 MHz, DMSO-d_6) δ: 10.0 (CH_3), 27.9 (CH_2), 28.9 (CH_2), 55.9 (CH_2), 69.9 (CH), 74.5 (C), 98.7 (C), 114.4 (C), 123.6 (C), 125.3 (CH), 128.1 (2 CH), 129.3 (2 CH), 131.1 (C), 134.2 (CH), 134.6 (CH), 138.8 (C), 139.1 (C), 142.8 (C). LC/MS ESI$^+$ t_R 2.88 min, (m/z) $[M+H]^+$ 447.51/448.78/450.54. HRMS (+ESI): 448.0728 (M + H^+). Calcd for $C_{20}H_{18}ClN_3O_5S$: 448.0728.

4.1.1.20. 1-{[6-Chloro-3-nitro-2-(phenylsulfonylmethyl)imidazo[1,2-*a*]pyridin-8-yl]ethynyl}cyclopentanol (23)

Compound **23** was obtained after purification by chromatography (eluent: dichloromethane/methanol 9.8/0.2) and recrystallization from propan-2-ol as a white solid in 61% yield (0.26 g). mp 214 °C. ^{1}H NMR (400 MHz, DMSO-d_6) δ: 1.68–1.81 (4H, m), 1.87–1.99 (4H, m), 5.27 (2H, s), 5.55 (1H, s), 7.59–7.63 (2H, m), 7.73–7.80 (3H, m), 8.05 (1H, d, J = 1.9 Hz), 9.30 (1H, d, J = 1.9 Hz). ^{13}C NMR (100 MHz, DMSO-d_6) δ: 23.1 (2 CH_2), 41.9 (2 CH_2), 55.9 (CH_2), 72.9 (C), 74.4 (C), 104.3 (C), 113.9 (C), 123.6 (C), 125.6 (CH), 128.1 (2 CH), 129.3 (2 CH), 131.2 (C), 134.2 (CH), 134.7 (CH), 138.8 (C), 139.2 (C), 142.5 (C). LC/MS ESI$^+$ t_R 3.35 min, (m/z) $[M+NH_4]^+$ 476.91/478.71. HRMS (+ESI): 460.0727 (M + H^+). Calcd for $C_{21}H_{18}ClN_3O_5S$: 460.0728.

4.1.1.21. 1-{[6-Chloro-3-nitro-2-(phenylsulfonylmethyl)imidazo[1,2-*a*]pyridin-8-yl]ethynyl}cyclohexanol (24)

Compound **24** was obtained after purification by chromatography (eluent: dichloromethane/methanol 9.6/0.4) and recrystallization from acetonitrile as a white solid in 77% yield (0.34 g). mp 232 °C. ^{1}H NMR (400 MHz, DMSO-d_6) δ: 1.26 (1H, bs), 1.49–1.65 (8H, m), 1.84–1.90 (2H, m), 5.25 (2H, s), 7.56–7.63 (2H, m), 7.71–7.80 (3H, m), 8.07 (1H, d, J = 1.83 Hz), 9.31 (1H, d, J = 1.81 Hz). ^{13}C NMR (100 MHz, DMSO-d_6) δ: 22.6 (2 CH_2), 24.8 (CH_2), 39.4 (2 CH_2), 56.0 (CH_2), 67.3 (C), 75.7 (C), 104.2 (C), 113.9 (C), 123.6 (C), 125.6 (CH), 128.0 (2 CH), 129.2 (2 CH), 131.2 (C), 134.1 (CH), 134.6 (CH), 138.8 (C), 139.3 (C), 142.5 (C). LC/MS ESI$^+$ t_R 3.58 min, (m/z) $[M+NH_4]^+$ 490.94/492.91. HRMS (+ESI): 474.0887 ($M + H^+$). Calcd for $C_{22}H_{20}ClN_3O_5S$: 474.0885.

4.1.1.22. Preparation of 4-[3-amino-6-chloro-2-(phenylsulfonylmethyl)imidazo[1,2-a]pyridin-8-yl]but-3-yn-1-ol (25)

A mixture of 8-bromo-6-chloro-3-nitro-2-(phenylsulfonylmethyl)imidazo[1,2-*a*]pyridine **4** (400 mg, 1 equiv.) in acetic acid (60 mL), iron powder (519 mg, 10 equiv.) was stirred and heated under reflux for 30 min. The mixture was then filtered through celite and the solvent was evaporated *in vacuo*. The resulting residue was diluted with H_2O and basified with saturated aqueous $NaHCO_3$. The mixture was extracted three times with dichloromethane, dried over $MgSO_4$, filtered and evaporated. Then, a mixture of the previous residue (200 mg, 1 equiv.), tetrakis(triphenylphosphine)palladium(0) (57.8 mg, 0.1 equiv.), copper iodide (9.5 mg, 0.1 equiv.), diisopropylamine (843 µL, 12 equiv.) and but-3-yn-1-ol (57 µL, 1.5 equiv.) in THF (7 mL) was stirred under N_2 at room temperature for 24 h. The reaction mixture was then slowly poured into an ice-water mixture. The resulting suspension was filtered. Compound **25** was obtained after purification by flash chromatography (eluent: dichloromethane/ethyl acetate 20/80) as a yellow solid in 57 % yield (111 mg). mp 190 °C. ^{1}H NMR (400 MHz, DMSO-d_6) δ: 2.63 (2H, t, J = 6.8 Hz), 3.60 (2H, dd, J = 10.6, 6.4 Hz), 4.79 (2H, s), 4.94 (1H, s), 5.28 (2H, s), 7.12 (1H, d, J = 1.8 Hz), 7.59 (2H, t, J = 7.7 Hz), 7.71 (1H, t, J = 7.4 Hz), 7.82 – 7.76 (2H, m), 8.20 (1H, d, J = 1.8 Hz). ^{13}C NMR (100 MHz, DMSO-d_6) δ: 23.6 (CH_2), 54.5 (CH_2), 59.6 (CH_2), 75.9 (CH), 95.2 (CH), 113.0 (C), 115.9 (CH), 117.5 (C), 120.0 (C), 124.8 (CH), 128.1 (2 CH), 129.0 (2 CH), 132.3 (C), 133.6 (C), 136.1 (CH), 139.5 (C). LC/MS ESI$^+$ t_R 1.86 min, (m/z) $[M+H]^+$ 390.02/392.02. HRMS (+ESI): 390.0671 $[M+H]^+$; Calcd for $C_{18}H_{16}ClN_3O_3S$: 390.0674.

4.1.2. Electrochemistry

Voltammetric measurements were carried out with a potentiostat Autolab PGSTAT100 (ECO Chemie, The Netherlands) controlled by GPES 4.09 software. Experiments were performed at room temperature in a homemade airtight three–electrode cell connected to a vacuum/argon line. The reference electrode consisted of a saturated calomel electrode (SCE) separated from the

solution by a bridge compartment. The counter electrode was a platinum wire of 1 cm^2 apparent surface. The working electrode was GC microdisk (1.0 mm of diameter – Bio-logic SAS). The supporting electrolyte (nBu_4N)[PF_6] (Fluka, 99% puriss electrochemical grade) and the solvent DMSO (Sigma-Aldrich puriss p.a. dried <0.02% water) were used as received and simply degassed under argon. The solutions used during the electrochemical studies were typically 10^{-3} M in compound and 0.1 M in supporting electrolyte. Before each measurement, the solutions were degassed by bubbling Ar and the working electrode was polished with a polishing machine (Presi P230). Under these experimental conditions employed in this work, the half-wave potential ($E_{1/2}$) of the ferrocene Fc+/Fc couple in DMSO was $E_{1/2}$ = 0.45 V vs SCE. Experimental peak potentials have been measured versus SCE and converted to NHE by adding 0.241 V.

4.2. Biology

4.2.1. Antileishmanial activity against *L. donovani* promastigotes

Leishmania species used in this study were *L. donovani* (MHOM/IN/00/DEVI) purchased from CNR Leishmania (Montpellier, France). *Leishmania* promastigotes forms were grown in Schneider's Drosophila medium (Life Technologies, Saint-Aubin, France) supplemented with 100 U/mL penicillin, 100 µg/mL streptomycin, 2 mM L-glutamine and 20% FCS (Life Technologies, Saint-Aubin, France) at 27 °C. The *in vitro* evaluation of the antileishmanial activity on promastigote forms of the tested compound was carried out by an MTT assay according to the protocol of Mosmann with some modifications. [29] Briefly, promastigotes in log-phase were incubated at an average density of 10^6 parasites/mL in sterile 96-well plates with various concentrations of compound dissolved in DMSO (final concentration less than 0.5% v/v), in duplicate. Appropriate controls treated by DMSO, miltefosine, amphotericin B, fexinidazole and doxorubicin (reference drugs purchased from Sigma-Aldrich, Saint-Louis, Missouri, USA) were added to each set of experiments. After a 72h incubation period at 27 °C, parasitic metabolic activity was determined. Each plate-well was then microscope-analyzed for detecting possible precipitate formation. 20 µL of MTT (3-(4,5-dimethylthiazol-2-yl)-2,5-diphenyltetrazolium bromide) (Sigma-Aldrich, Saint-Louis, Missouri, USA) solution (5 mg/mL in PBS) were added to each well followed and incubated 4 h at 27 °C. The enzyme reaction was then stopped by addition of 100 µL of 50% isopropanol – 10% sodium dodecyl sulfate. Plates were shaken vigorously at 300 rpm for 10 min. The absorbance was finally measured at 570 nm in a BIO-TEK Elx808 (Biotek, Colmar, France) absorbance microplate reader. Inhibitory concentration 50% (EC_{50}) was defined as the concentration of drug required to inhibit by 50% the metabolic activity of *Leishmanial* promastigotes forms compared to the control. EC_{50} were calculated by non-linear

regression analysis processed dose-response curves, using TableCurve 2D V5.0 software. EC_{50} values represent the mean value calculated from at least three independent experiments.

4.2.2. Antileishmanial activity on *L. infantum* axenic amastigotes [30]

L. infantum promastigotes (MHOM/MA/67/ITMAP-263, CNR Leishmania, Montpellier, France, expressing luciferase activity) were cultivated in RPMI 1640 medium supplemented with 10% foetal calf serum (FCS), 2 mM L-glutamine and antibiotics (100 U/mL penicillin and 100 µg/mL streptomycin) and harvested in logarithmic phase of growth by centrifugation at 900 g for 10 min. The supernatant was removed carefully and was replaced by the same volume of RPMI 1640 complete medium at pH 5.4 and incubated for 24 h at 24 °C. The acidified promastigotes were then incubated for 24 h at 37 °C in a ventilated flask to transform promastigotes into axenic amastigotes. The amastigote stage was checked both by electron microscopy (short flagellum with small bulbous tip extending beyond a spherical cell body) and RT-PCR for confirming the overexpression of ATG8 and amastin genes in amastigotes, compared to promastigotes. The effects of the tested compounds on the growth of *L. infantum* axenic amastigotes were assessed as follows. *L. infantum* amastigotes were incubated at a density of 2×10^6 parasites/mL in sterile 96-well plates with various concentrations of compounds dissolved in DMSO (final concentration less than 0.5% v/v), in duplicate. Appropriate controls DMSO, amphotericin B, miltefosine and fexinidazole (reference drugs purchased from Sigma Aldrich) were added to each set of experiments. After a 48 h incubation period at 37 °C, each plate-well was then microscopically-examined to detect any precipitate formation. To estimate the luciferase activity of axenic amastigotes, 80 µL of each well were transferred to white 96-well plates, Steady Glow® reagent (Promega) was added according to manufacturer's instructions, and plates were incubated for 2 min. The luminescence was measured in Microbeta Luminescence Counter (PerkinElmer). Efficient concentration 50% (EC_{50}) was defined as the concentration of drug required to inhibit by 50% the metabolic activity of *L. infantum* amastigotes compared to control. EC_{50} values were calculated by non-linear regression analysis processed on dose response curves, using TableCurve 2D V5 software. EC_{50} values represent the mean of three independent experiments.

4.2.3. Antitrypanosomal evaluation on *T. b. brucei* BSF trypomastigotes

The effects of the tested compounds on the growth of *T. b. brucei* were assessed by Alamar Blue® assay described by Räz *et al*. [31] *T. b. brucei* AnTat 1.9 (IMTA, Antwerpen, Belgium) was cultured in MEM with Earle's salts, supplemented according to the protocol of Baltz *et al*. [32] with the following modifications: 0.5 mM mercaptoethanol (Sigma Aldrich®, France), 1.5 mM L-cysteine (Sigma Aldrich®), 0.05 mM bathocuproïne sulfate (Sigma Aldrich®) and 20% heat-inactivated horse serum (Gibco®, France), at 37 °C and 5% CO_2. They were incubated at an

average density of 2000 parasites/100 µL in sterile 96-wells plates (Fisher®, France) with various concentrations of compounds dissolved in DMSO, in duplicate. Appropriate controls treated by DMSO on sterile water, suramin, eflornithine and fexinidazole (reference drugs purchased from Sigma Aldrich, France and Fluorochem, UK) were added to each set of experiments. After a 69 h incubation period at 37 °C, 10 µL of the viability marker Alamar Blue® (Fisher, France) was then added to each well, and the plates were incubated for 5 h. The plates were read in a ENSPIRE microplate reader (PerkinElmer) using an excitation wavelength of 530 nm and an emission wavelength of 590 nm. EC_{50} was defined as the concentration of drug necessary to inhibit by 50% the activity of *T. b. brucei* compared to the control. EC_{50} were calculated by nonlinear regression analysis processed on dose-response curves, using GraphPad Prism software (USA). EC_{50} values were calculated from three independent experiments.

4.2.4. Antitrypanosomal evaluation on the development of *T. cruzi* amastigotes

Vero cells (normal kidney epithelial cells of *Cercopithecus aethiops*) were obtained from the Virology Laboratory of the Pitié Salpêtrière Hospital (Paris, France). At late exponential growth phase, trypsin-treated Vero cells were subcultured every seven days in RPMI-1640 medium (Life technologies) supplemented with streptomycin/penicillin (Life technologies) and 5% heat-inactivated fœtal bovine serum (FBS) (Life technologies). Subcultures were maintained at 37 °C in a humidified atmosphere of 5% CO_2. CL Brener strain (collection number: MNHN-CEU- 2016-0159) was a gift from Pr. P. Grellier of the Muséum National d'Histoire Naturelle (Paris, France). *T. cruzi* stocks were maintained by weekly passage in Vero cells. Infectious trypomastigotes were collected from culture supernatants.

Then, sterile, 6-well plates were seeded with exponentially growing Vero cells (40,000 cells per cm^2 in 2, 2 mL RPMI with serum per well) harvested from the preceding subcultures, were added to each well. After incubation at 37 °C for 2 days in 5% CO_2 in air, the cells were infected with *T. cruzi* trypomastigotes in ratio 3:1 (parasites : host cells). After 24 h, the non-infecting trypomastigotes removed by washing twice with HBSS buffer (without Ca^{2+} and Mg^{2+}) and the chemical compounds in completed RPMI media were added immediately, to be tested to their inhibitory effects on parasite growth and development. Culture plates were incubated for an additional 120 h at 37 °C with 5% CO_2.Three replicate wells for each condition were done. On days 5 and 6 post-infection, trypomastigotes were released from the cells. On day 6, the culture medium was removed and transferred to a centrifuge tube. Attached infected cells were washed with 5 mL of HBSS buffer. The culture medium and wash containing trypomastigotes were mixed and centrifuged at 1000 g for 15 min at room temperature. Subsequently, trypomastigotes re-suspended in 2 mL and counted in a haemocytometer (Kova cells) using a light microscope. For 50% effective concentration (EC_{50}) determinations, compounds were serially diluted 2 to 4-fold

in RPMI media, with final assay concentrations ranging from 0.1 to 25 µM. The 50% inhibiting concentrations (EC_{50}), defined as the drug concentration that resulted in a 50% reduction of trypomastigotes compared to the non-treated controls was estimated by non-linear regression analysis. EC_{50} values represent the mean value calculated from two independent experiments that were performed in triplicate.

4.2.5. Antileishmanial activity on *L. donovani* promastigotes NTR1 and NTR2 over-expressing strain.

The clonal *Leishmania donovani* cell line LdBOB (derived from MHOM/SD/62/1S-CL2D) was grown as promastigotes at 26 °C in modified M199 media, as previously described [33]. LdBOB promastigotes overexpressing NTR1 (LinJ.05.0660) [16] and NTR2 (LinJ.12.0730) [17] were grown in the presence of nourseothricin (100 µg/mL). To examine the effects of test compounds on growth, triplicate promastigote cultures were seeded with 5×10^4 parasites/mL. Parasites were grown in 10 mL cultures in the presence of drug for 72 h, after which 200 µL aliquots of each culture were added to 96-well plates, 50 µM resazurin was added to each well and fluorescence (excitation of 528 nm and emission of 590 nm) measured after a further 4 h incubation [15]. Data were processed using GRAFIT (version 5.0.4; Erithacus software) and fitted to a 2-parameter equation, where the data are corrected for background fluorescence, to obtain the effective concentration inhibiting growth by 50% (EC_{50}):

$$y = \frac{100}{1 + \left(\frac{[I]}{EC_{50}} \right)^m}$$

In this equation, [I] represents inhibitor concentration and m is the slope factor. Experiments were repeated at least two times and the data is presented as the mean plus standard deviation.

4.2.6 Antitrypanosomal activity on *T. brucei* NTR1 over-expressing strain.

Trypanosoma brucei bloodstream-form 'single marker' S427 (T7RPOL TETR NEO) and drug-resistant cell lines were cultured at 37 °C in HMI9-T medium [34] supplemented with 2.5 µg/mL G418 to maintain expression of T7 RNA polymerase and the tetracycline repressor protein. Bloodstream trypanosomes overexpressing the *T. brucei* nitroreductase (NTR1) [35] were grown in medium supplemented with 2.5 µg/mL phleomycin and expression of NTR was induced by the addition of 1 µg/mL tetracycline. Cultures were initiated with 1×10^5 cells/mL and sub-cultured when cell densities approached 1–2 ($\times 10^6$)/mL.

In order to examine the effects of inhibitors on the growth of these parasites, triplicate cultures containing the inhibitor were seeded at 1×10^5 trypanosomes/mL. Cells overexpressing NTR were induced with tetracycline 48 h prior to EC_{50} analysis. Cell densities were determined after culture

for 72 h, as previously described [36]. EC_{50} values were determined using the following two-parameter equation by non-linear regression using GRAFIT:

where the experimental data were corrected for background cell density and expressed as a percentage of the uninhibited control cell density.

$$y = \frac{100}{1 + \left(\frac{[I]}{EC_{50}} \right)^{m}}$$

In this equation, [I] represents inhibitor concentration and m is the slope factor.

4.2.7. Cytotoxicity evaluation on HepG2 cell line

HepG2 cell line was maintained at 37 °C, 6% CO_2 with 90% humidity in RPMI supplemented with 10% fœtal bovine serum, 1% L-glutamine (200 mM) and penicillin (100 U/mL)/streptomycin (100 mg/mL) (complete RPMI medium). The evaluation of the tested molecules cytotoxicity on the HepG2 (hepatocarcinoma cell line purchased from ATCC, ref HB-8065) cell line was performed according to the method of Mosmann [29] with slight modifications. Briefly, 5×10^3 cells in 100 mL of complete medium were inoculated into each well of 96-well plates and incubated at 37 °C in a humidified 6% CO_2. After 24 h incubation, 100 mL of medium with various product concentrations dissolved in DMSO (final concentration less than 0.5% v/v) were added and the plates were incubated for 72 h at 37 °C. Triplicate assays were performed for each sample. Each plate-well was then microscope-examined for detecting possible precipitate formation before the medium was aspirated from the wells. 100 mL of MTT (3-(4,5-dimethyl-2-thiazolyl)-2,5-diphenyl-2*H*-tetrazolium bromide) solution (0.5 mg/mL in medium without FCS) were then added to each well. Cells were incubated for 2 h at 37 °C. After this time, the MTT solution was removed and DMSO (100 mL) was added to dissolve the resulting blue formazan crystals. Plates were shaken vigorously (700 rpm) for 10 min. The absorbance was measured at 570 nm with 630 nm as reference wavelength using a BIO-TEK ELx808 Absorbance Microplate Reader. DMSO was used as blank and doxorubicin (purchased from Sigma Aldrich) as positive control. Cell viability was calculated as percentage of control (cells incubated without compound). The 50% cytotoxic concentration (CC_{50}) was determined from the dose–response curve by using the TableCurve 2D v.5.0 software (Jandel scientific). CC_{50} values represent the mean value calculated from three independent experiments.

4.2.8. Cytotoxicity on THP-1 cell line

The evaluation of the tested molecules cytotoxicity on the THP-1 cell line (acute monocytic leukemia cell line purchased from ATCC, ref TIB-202) was performed according to the method of Mosman [29] with slight modifications. Briefly, cells in 100 µL of complete RPMI medium,

were incubated at an average density of 5×10^4 cells/mL in sterile 96-well plates with various concentrations of compounds dissolved in DMSO (final concentration less than 0.5% v/v), in duplicate. The plates were incubated for 72 h at 37 °C. Each well plate was then microscope-examined for detecting possible precipitate formation before the medium was aspirated from the wells. 100 µL of MTT solution (0.5 mg/mL in medium without FCS) were then added to each well. Cells were incubated for 2 h at 37 °C. After this time, the MTT solution was removed and DMSO (100 µL) was added to dissolve the resulting blue formazan crystals. Plates were shaken vigorously (300 rpm) for 10 min. The absorbance was measured at 570 nm with 630 nm as reference wavelength spectrophotometer using a BIO-TEK ELx808 Absorbance Microplate Reader. DMSO was used as blank and doxorubicin (purchased from Sigma Aldrich) as positive control. Cell viability was calculated as percentage of control (cells incubated without compound). The 50% cytotoxic concentration (CC_{50}) was determined from the dose–response curve by using the TableCurve 2D v.5.0 software. CC_{50} values represent the mean value calculated from three independent experiments.

4.2.9. Ames test

Mutagenicity test was carried out by using a modified version of the liquid incubation assay of the classical Ames test [37]. *S. typhimurium* tester strains (TA97a, TA98, TA100 and TA102) were grown overnight in a Nutrient Broth n°2 (Oxoid, France). After this period, 5 - 50 mM DMSO solutions of the tested drugs were added to 0.1 mL of culture and incubated with 4% S9 mix for 1 h at 37 °C with shaking. Each sample was assayed in duplicate. After incubation, 2 mL of molten top agar were mixed gently with the pre-incubated solution and poured onto Vogel-Bonner minimal agar plates. After 48 h at 37 °C in the dark, the number of spontaneous and drug induced revertants per plate was determined for each dose with a laser bacterial colony counter. A product was considered mutagenic when it induces a two-fold increase of the number of revertants compared with the spontaneous frequency (negative control). For each *Salmonella* strain, a positive- (using benzo[*a*]pyrene) and solvent-control were performed with S9mix.

4.2.10. Comet assay

The alkaline comet assay was used to detect DNA strand breaks and alkali-labile sites. Trypsinized HepG2 cells were embedded in 0.7% low-melting point agarose (Sigma “Low Gelling Temperature”) and laid on pre-cut sheets of polyester film (Gelbond® film) to perform minigel deposits as previously described [38]. Film were then placed in lysis solution (NaCl 2.5 M, Na_2EDTA 0.1 M, Tris 10 mM, 1 % Triton X-100, 10 % DMSO pH 10) for 18h at 4 °C. Electrophoresis (with a solution which contained 0.3 M NaOH, 1 mM Na_2EDTA, pH > 13) was processed for 24 min in a tank with a power supply giving 28 V (resulting in 0.8 V/cm). After

electrophoresis, films were immersed 2 × 5 min in PBS for neutralization, followed by fixation in 100% ethanol for 1.5 h and drying. After staining with SYBR® Gold (Life Technologies) at 10 000 X dilution for 20 min, films were observed at 20 × magnification with an epifluorescence microscope equipped with an automated platform (Nikon NiE) and coupled to a camera (DS-Q1Mc) and the software Nikon NiS Element Advanced Research to automatically capture images. In these images, for each cell, the level of DNA damage was evaluated using a semi-automated scoring system, by measurement of the intensity of all tail pixels divided by the total intensity of all pixels in head and tail of comet, by means of the software "Lucia comet assay" (Laboratory Imaging, Prague Czech Republic). Fifty cells per deposit and three deposits per sample were analyzed. The median from these values was calculated, and named "% tail DNA".

4.3. *In vitro* Pharmacokinetic and physicochemical studies

4.3.1. Plasma protein binding procedure

Plasma doped with the tested compound is incubated at 37 °C in triplicate in one of the compartments of the insert, the other compartment containing a phosphate buffer solution at pH 7.2. After stirring for 4 h at 300 rpm, a 25 µL aliquot of each compartment is taken and diluted; the dilution solution is adapted to obtain an identical matrix for all the compartments after dilution. In parallel, the reprocessing of a plasma doped but not incubated will allow to evaluate the recovery of the study. The LC-MS used for this study is a Waters® Acquity I-Class / Xevo TQD, equipped with a Waters® Acquity BEH C18 column, 50 × 2.1 mm, 1.7 µM. The mobile phases are (A) ammonium acetate 10 mM and (B) acetonitrile with 0.1% formic acid. The injection volume is 1 µL and the flow rate is 600 µL/min. The chromatographic analysis, total duration of 4 min, is made with the following gradient: 0 < t < 0.2 min, 2% (B); 0.2 < t < 2 min, linear increase to 98% (B); 2 < t < 2.5 min, 98% (B); 2.5 < t < 2.6 min, linear decrease to 2% (B); 2.6 < t < 4 min, 2% (B). Carbamazepine, oxazepam, warfarin and diclofenac are used as reference drugs and propranolol is used as internal standard. The unbound fraction (f_u) is calculated according to the following formula: $f_u = \frac{A_{Plasma,4h} - A_{PBS,4h}}{A_{Plasma,4h}} \times 100$. The percentage of recovery is calculated according to the following formula:

$$\%\ \mathbf{Recovery} = \frac{\left(\mathbf{V_{PBS}} \times \mathbf{A_{PBS,4h}}\right) + \left(\mathbf{V_{Plasma}} \times \mathbf{A_{Plasma,4h}}\right)}{\left(\mathbf{V_{Plasma}} \times \mathbf{A_{Plasma,0h}}\right)}$$

Where A is the ratio of the area under peak of the studied molecule and the area under peak of the internal standard (propranolol 200 nM). V is the volume of solution present in the compartments (V_{PBS} = 350 µL and V_{plasma} = 200 µL).

4.3.2. Microsomal stability protocol

The tested product and propranolol, used as reference, are incubated in duplicate (reaction volume of 0.5 mL) with female mouse microsomes (CD-1, 20 mg/mL, BD Gentest™) at 37 °C in a 50 mM phosphate buffer, pH 7.4, in the presence of $MgCl_2$ (5 mM), NADP (1 mM), glucose-6-phosphate dehydrogenase (0.4 U/mL) and glucose-6-phosphate (5 mM). For the estimation of the intrinsic clearance: 50 µL aliquot at 0, 5, 10, 20, 30 and 40 min are collected and the reaction is stopped with 4 volumes of acetonitrile (ACN) containing the internal standard. After centrifugation at 10000 g, 10 min, 4 °C, the supernatants are kept at 4 °C for immediate analysis or placed at -80 °C in case of postponement of the analysis. Controls (t_0 and t_{final}) in triplicate are prepared by incubation of the internal standard with microsomes denatured by acetonitrile. The LC-MS used for this study is a Waters® Acquity I-Class / Xevo TQD, equipped with a Waters® Acquity BEH C18 column, 50 × 2.1 mm, 1.7 µm. The mobile phases are (A) ammonium acetate 10 mM and (B) acetonitrile with 0.1% formic acid. The injection volume is 1 µL and the flow rate is 600 µL/min. The chromatographic analysis, total duration of 4 min, is made with the following gradient: $0 < t < 0.2$ min, 2% (B); $0.2 < t < 2$ min, linear increase to 98% (B); $2 < t < 2.5$ min, 98% (B); $2.5 < t < 2.6$ min, linear decrease to 2% (B); $2.6 < t < 4$ min, 2% (B). 8-Bromo-6-chloro-3-nitro-2-(phenylsulfonylmethyl)imidazo[1,2-*a*]pyridine is used as internal standard. The quantification of each compound is obtained by converting the average of the ratios of the analyte/internal standard surfaces to the percentage of consumed product. The ratio of the control at t_0 corresponds to 0% of product consumed. The calculation of the half-life ($t_{1/2}$) of each compound in the presence of microsomes is done according to the equation: $t_{\frac{1}{2}} = \frac{\ln(2)}{k}$, where k is the first-order degradation constant (the slope of the logarithm of compound concentration versus incubation time). The intrinsic clearance *in vitro* (Cl_{int} expressed in µL/min/mg) is calculated according to the equation:

$$Cl_{int} = \frac{\frac{dose}{AUC_\infty}}{[microsomes]}$$

Where dose is the initial concentration of product in the sample, AUC_∞ is the area under the concentration-time curve extrapolated to infinity and [microsomes] is the microsome concentration expressed in mg/µL.

4.3.3. Blood brain barrier parallel artificial membrane permeability assay (BBB-PAMPA)

The BBB-Pampa experiments were conducted using the Pampa Explorer Kit (Pion Inc) according to manufacturer's protocol. Briefly, the stock compound solution (20 mM in DMSO) was diluted in Prisma HT buffer pH 7.4 (pION) to 100 µM. 200 µL of this solution (n = 6) was added to donor plate (P/N 110243). 5 µL of the BBB-1 Lipid (P/N 110672) was used to coat the membrane filter

of the acceptor plate (P/N 110243). 200 µL of the Brain Sink Buffer (P/N 110674) was added to each well of the acceptor plate. The sandwich was incubated at room temperature for 4 h, without stirring. After the incubation the UV-visible spectra were measured with the microplate reader (Tecan infinite M200) and the permeability value (P_e) was calculated by the PAMPA Explorer software v.3.7 (pION). Corticosterone (P_e = 138.6 ± 22.0 nm/s), and theophylline (P_e = 5.5 ± 0.3 nm/s) were used as high and low permeability standards, respectively. Each measure was performed in sixplicate.

4.3.4. Thermodynamic solubility at pH 7.4 of compound 19

Thermodynamic solubility at pH 7.4 of compounds was determined according to a miniaturized shake-flask method (Organisation for Economic Cooperation and Development guideline n°105) [39]. Phosphate Buffer solutions (pH 7.4, 10 µM, ionic strength 150 µM) were prepared from Na_2HPO_4, KH_2PO_4 and KCl (Sigma Aldrich, Saint Quentin Fallavier, France); 10 µL of 20 mM stock solution were added to 5 mL glass tube containing 990 mL buffer (n = 3). Tubes were briefly sonicated and shacked by inversion during 24 h at room temperature. Then, tube contents were put in a microtube which was centrifuged at 12,225 g for 10 min; 100 µL supernatant was mixed with 100 µL acetonitrile in a Greiner UV microplate. Standard solutions were prepared extemporaneously diluting 20 mM DMSO stock solutions at 0, 5, 10 and 20 mM; 5 µL each working solution was diluted with 995 µL buffer and 100 µL was then mixed in microplate with 100 µL acetonitrile to keep unchanged the final proportions of each solvent in standard solutions and samples. Determination of solubility at pH 7.4 was made with an Infinite M200Pro (Tecan, Lyon, France) microplate reader in spectrophotometric mode (230 to 450 nm) from the specific λ_{max} of each compound. The calibration curve obtained from the three standard solutions of tested compounds at 0, 25, 50, and 100 µM in a 50:50 (vol/vol) mixture of buffer with acetonitrinile/DMSO (99:1; vol/vol). Calibration curves were linear with $R^2 > 0.99$.

4.4. *In vivo* studies

Female Swiss mice of 8 weeks (weight 30-32 g) are used. All animals were kept under the same conditions according to laboratory animal care guidelines (European convention SPE123), and all protocols were approved by the ethical committee and the Ministry of Higher Education, Research and Innovation with the agreement number APAFIS#19730-2019031215178087 v1.

The determination of maximal tolerated dose used one group of 4 mice which received an oral administration (intragastrical gavage) of **15** at 100 mg/kg. **15** was prepared as a suspension comprising 5% Tween 80/ 95% carboxymethylcellulose 0.5% in water.

Observations of side effects were codified. The same protocol was used with repeated dose during 5 days.

4.4.1. Chemicals

The internal standard (IS), ornidazole, was obtained from Sigma Aldrich. LC-MS Optima grade Acetonitrile (ACN) and Methanol (MeOH), acetic acid and formic acid (FA) were purchased from Fisher Scientific. Ready-to-use QuEChERS salts (6 g $MgSO_4$/1.5 g NaCl/1.5 g sodium citrate dihydrate/750 mg sodium citrate sesquihydrate) were supplied by VWR**.**

4.4.2. Sample preparation

Samples were stored at -20 °C until extraction. 200 µL of ACN containing ornidazole (internal standard; IS) at a concentration of 625 ng/mL were added to 100 µL blood samples. The mixture was vortexed during 30 sec. After 10 min, 40 mg of QuEChERS salts were added. Samples were briefly vortexed and centrifuged at 16,000 g for 10 min. Ten microliters of the upper layer was directly transferred in an injection vial before being diluted (1/10; v/v) in a 0.1 % formic acid in water. Finally, 5µL was injected in the LC-MS-MS system. Calibrations standards (9 levels, from 5 to 1,000 ng/mL) and quality controls (QC) (10, 75 and 625 ng/mL) were obtained by adding appropriate 20 × working standard solutions in blank whole blood.

4.4.3. LC-MS/MS conditions

The chromatographic system consisted in two Shimadzu LC-30 AD pumps (NexeraX2), a CTO 20AC oven, and a SIL-30AC autosampler (Shimadzu, Marne-la-Vallée, France). Chromatographic separation was performed using a EC-C8 column (Poroshell 120, 2.1 mm × 75 mm, 2.7 µM; Agilent) at a flow rate of 0.25 mL/min using a gradient of 0.1% acetic acid in water (A) and 0.1% acetic acid in MeOH/ACN 50:50 (B) programmed as follows: 0.0–0.1, 20% (B); 0.1–1.0, 20 to 70% (B); 1.0–4.0, 70% to 100% (B); 4.0–5.5, 100% (B); 5.5–6.0, 100 to 20% (B); and 6.0–8.0 column equilibration with 20% (B). Oven temperature was set at 60 °C.

A Shimadzu 8060 triple quadrupole mass spectrometer was used in the positive electrospray ionization mode. The main common parameter settings were as follows: interface voltage, 1.5 kV; nebulizing gas flow, 3 L/min; heating gas flow, 10 L/min; interface temperature, 300 °C; desolvatation line (DL) temperature, 250 °C; heat block temperature, 400 °C; and drying gas flow, 10 L/min. All parameters (collision energy, Q1/Q3 pre-bias) were optimized from standard flow injection analysis. Dwell time was set at 100 ms per transition.

4.4.4. Validation procedure for whole blood

Validation protocol and the set of acceptance criteria were as follows:

- Linearity: Calibration curve was generated by plotting the peak area ratios (analyte/internal standard) vs the expected concentration. Linearity of the calibration curve was evaluated by a quadratic regression analysis using a $1/x^2$ weighting. A value greater than 0.99 was expected for the coefficient of determination (r^2).
- Precision and accuracy of the method were assessed at lower limit of quantitation (LLOQ; 5 ng/mL) and at the two quality control concentrations (10, 75 and 625 ng/mL). Precision is calculated as the coefficient of variation (CV%) within a single run (intra-assay; n = 5) and between different assays (inter-assay; n = 5), and accuracy is the percentage of deviation between nominal and found concentration with the established calibration curve. Acceptance criteria were intra-assay and inter-assay precision (CV%) and an accuracy (bias) less than 20%.
- The lower limit of quantification (LLOQ) was estimated to be the minimal concentration with accuracy and precision within ± 20%. The lower limit of detection (LLOD) was calculated based on a signal-to-noise ratio >3.
- Extraction recoveries were determined by comparing the LLOQ and the quality controls samples (n = 5) with their extracted blank whole blood counterparts spiked at the correct concentration after extraction (n = 3). CV% in the extraction recovery had to be less than 20%.
- The effect of dilution was investigated on samples spiked at MQC and HQC then analyzed after 1.25-, two- and four-fold dilutions. Precision CV and bias were set less than 25% to successfully validate.
- The absence of carryover was checked by injecting blank samples just after the analysis of the most concentrated sample (1,000 ng/mL).

4.4.5. Pharmacokinetics

The same samples used for the validation were used for the analysis. Monolix Lixoft software was used to analyze data by noncompartmental model to fit pharmacokinetics parameters.

Acknowledgement

This work was supported by Aix-Marseille Université, the Université de Toulouse and the CNRS. A. Fairlamb and S. Wyllie are supported by funding from the Wellcome Trust (WT105021). C. Fersing thanks the Assistance Publique - Hôpitaux de Marseille (AP-HM) for hospital appointment. J. Pedron thanks the Université Paul Sabatier and the Conseil Régional Occitanie for PhD funding. The authors thank Dr Vincent Remusat for the NMR spectra recording, Dr Christophe Chendo and Dr Valérie Monnier for the HRMS analyses and Dr Michel Giorgi for the X-ray structure determinations. Catherine Piveteau from Institut Pasteur de Lille is also

acknowledged for her contribution in determining *in vitro* PK parameters. We thank Dr Jean-Baptiste Woillard for the *in vivo* pharmacokinetic analysis and Mr François-Ludovic Sauvage for his help in spectrometry analysis.

References

[1] D.H. Molyneux, L. Savioli, D. Engels, Neglected tropical diseases: progress towards addressing the chronic pandemic, The Lancet 389 (2017) 312–325, https://doi.org/10.1016/S0140-6736(16)30171-4.

[2] S. Burza, S.L. Croft, M. Boelaert, Leishmaniasis, The Lancet 392 (2018) 951–970, https://doi.org/10.1016/S0140-6736(18)31204-2.

[3] P. Büscher, G. Cecchi, V. Jamonneau, G. Priotto, Human african trypanosomiasis, The Lancet 390 (2017) 2397–2409, https://doi.org/10.1016/S0140-6736(17)31510-6.

[4] J.A. Pérez-Molina, I. Molina, Chagas disease, The Lancet 391 (2018) 82–94, https://doi.org/10.1016/S0140-6736(17)31612-4.

[5] (a) World Health Organization (WHO), Neglected tropical diseases, http://www.who.int/neglected_diseases/diseases/en/ (accessed March 10th 2020). (b) World Health Organization (WHO), Health statistics and information systems, http://www.who.int/healthinfo/global_burden_disease/en/ (accessed March 10th 2020). (c) World Health Organization (WHO), Chagas disease (American trypanosomiasis), http://www.who.int/chagas/en/ (accessed March 10th 2020).

[6] (a) E.D. Deeks, Fexinidazole: first global approval, Drugs 79 (2019) 215–220, https://doi.org/10.1007/s40265-019-1051-6. (b) A.H. Fairlamb, Fexinidazole for the treatment of human African trypanosomiasis, Drug Today 55 (2019) 705–712, https://doi.org/10.1358/dot.2019.55.11.3068795

[7] DNDi, Drugs for Neglected Diseases Initiative research and development portfolio, https://www.dndi.org/diseases-projects/portfolio/ (accessed March 10th 2020).

[8] M.C. Field, D. Horn, A.H. Fairlamb, M.A.J. Ferguson, D.W. Gray, K.D. Read, M. De Rycker, L.S. Torrie, P.G. Wyatt, S. Wyllie, I.H. Gilbert, Anti-trypanosomatid drug discovery: an ongoing challenge and a continuing need, Nat. Rev. Microbiol. 15 (2017) 217–231, https://doi.org/10.1038/nrmicro.2016.193.

[9] S.P.S. Rao, M.P. Barrett, G. Dranoff, C.J. Faraday, C.R. Gimpelewicz, A. Hailu, C.L. Jones, J.M. Kelly, J.K. Lazdins-Helds, P. Mäser, J. Mengel, J.C. Mottram, C.E. Mowbray, D.L. Sacks, P. Scott, G.F. Späth, R.L. Tarleton, J.M. Spector, Drug discovery for kinetoplastid diseases: future directions, ACS Infect. Dis. 5 (2019) 152–157, https://doi.org/10.1021/acsinfecdis.8b00298.

[10] A. Buschini, L. Ferrarini, S. Franzoni, S. Galati, M. Lazzaretti, F. Mussi, C. Northfleet de Albuquerque, T. Maria Araújo Domingues Zucchi, P. Poli, Genotoxicity revaluation of three commercial nitroheterocyclic drugs: nifurtimox, benznidazole, and metronidazole, J. Parasitol. Res. 2009 (2009) 1–11, https://doi.org/10.1155/2009/463575.

[11] A.H. Fairlamb, S. Patterson, Current and future prospects of nitro-compounds as drugs for trypanosomiasis and leishmaniasis, Curr. Med. Chem. 26 (2018) 4454–4475, https://doi.org/10.2174/0929867325666180426164352.

[12] K. Nepali, H.-Y. Lee, J.-P. Liou, Nitro-group-containing drugs, J. Med. Chem. 62 (2019) 851–2893, https://doi.org/10.1021/acs.jmedchem.8b00147.

[13] A. Azam, M.N. Peerzada, K. Ahmad, Parasitic diarrheal disease: drug development and targets, Front. Microbiol. 6 (2015) 1183, https://doi.org/10.3389/fmicb.2015.01183.

[14] A.A. Voak, V. Gobalakrishnapillai, K. Seifert, E. Balczo, L. Hu, B.S. Hall, S.R. Wilkinson, An essential type I nitroreductase from *Leishmania major* can be used to activate leishmanicidal prodrugs, J. Biol. Chem. 288 (2013) 28466–28476, https://doi.org/10.1074/jbc.M113.494781.

[15] S. Wyllie, S. Patterson, L. Stojanovski, F.R.C. Simeons, S. Norval, R. Kime, K.D. Read, A.H. Fairlamb, The anti-trypanosome drug fexinidazole shows potential for treating visceral leishmaniasis, Sci. Transl. Med. 4 (2012) 119re1-119re1, https://doi.org/10.1126/scitranslmed.3003326.

[16] S. Wyllie, S. Patterson, A.H. Fairlamb, Assessing the essentiality of *Leishmania donovani* nitroreductase and its role in nitro drug activation, Antimicrob. Agents Chemother. 57 (2013) 901–906, https://doi.org/10.1128/AAC.01788-12.

[17] S. Wyllie, A.J. Roberts, S. Norval, S. Patterson, B.J. Foth, M. Berriman, K.D. Read, A.H. Fairlamb, Activation of bicyclic nitro-drugs by a novel nitroreductase (NTR2) in *Leishmania*, PLOS Pathog. 12 (2016) e1005971, https://doi.org/10.1371/journal.ppat.1005971.

[18] S. Patterson, S. Wyllie, L. Stojanovski, M.R. Perry, F.R.C. Simeons, S. Norval, M. Osuna-Cabello, M. De Rycker, K.D. Read, A.H. Fairlamb, The R enantiomer of the antitubercular drug PA-824 as a potential oral treatment for visceral leishmaniasis, Antimicrob. Agents Chemother. 57 (2013) 4699–4706, https://doi.org/10.1128/AAC.00722-13.

[19] B.S. Hall, C. Bot, S.R. Wilkinson, Nifurtimox activation by trypanosomal type I nitroreductases generates cytotoxic nitrile metabolites, J. Biol. Chem. 286 (2011) 13088–13095, https://doi.org/10.1074/jbc.M111.230847.

[20] B.S. Hall, S.R. Wilkinson, Activation of benznidazole by trypanosomal type I nitroreductases results in glyoxal formation, Antimicrob. Agents Chemother. 56 (2012) 115–123, https://doi.org/10.1128/AAC.05135-11.

[21] C. Castera-Ducros, L. Paloque, P. Verhaeghe, M. Casanova, C. Cantelli, S. Hutter, F. Tanguy, M. Laget, V. Remusat, A. Cohen, M.D. Crozet, P. Rathelot, N. Azas, P. Vanelle, Targeting the human parasite *Leishmania donovani*: discovery of a new promising anti-infectious pharmacophore in 3-nitroimidazo[1,2-*a*]pyridine series, Bioorg. Med. Chem. 21 (2013) 7155−7164, https://doi.org/10.1016/j.bmc.2013.09.002.

[22] C. Fersing, C. Boudot, J. Pedron, S. Hutter, N. Primas, C. Castera-Ducros, S. Bourgeade-Delmas, A. Sournia-Saquet, A. Moreau, A. Cohen, G. Pratviel, M.D. Crozet, S. Wyllie, A.H. Fairlamb, A. Valentin, P. Rathelot, N. Azas, B. Courtioux, P. Verhaeghe, P. Vanelle, 8-Aryl-6-chloro-3-nitro-2-(phenylsulfonylmethyl)imidazo[1,2-*a*]pyridines as potent antitrypanosomatid molecules bioactivated by type 1 nitroreductases, Eur. J. Med. Chem. 157 (2018) 115−126, https://doi.org/10.1016/j.ejmech.2018.07.064

[23] C. Fersing, L. Basmaciyan, C. Boudot, J. Pedron, S. Hutter, A. Cohen, C. Castera-Ducros, N. Primas, M. Laget, M. Casanova, S. Bourgeade-Delmas, M. Piednoel, A. Sournia-Saquet, V. Belle Mbou, B. Courtioux, E. Boutet-Robinet, M. Since, R. Milne, S. Wyllie, A.H. Fairlamb, A. Valentin, P. Rathelot, P. Verhaeghe, P. Vanelle, N. Azas, Nongenotoxic 3-nitroimidazo[1,2-*a*]pyridines are NTR1 substrates that display potent *in vitro* antileishmanial activity, ACS Med. Chem. Lett. 10 (2019) 34–39, https://doi.org/10.1021/acsmedchemlett.8b00347.

[24] C. Kieffer, A. Cohen, P. Verhaeghe, L. Paloque, S. Hutter, C. Castera-Ducros, M. Laget, S. Rault, A. Valentin, P. Rathelot, N. Azas, P. Vanelle, Antileishmanial pharmacomodulation in 8-nitroquinolin-2(1*H*)-one series, Bioorg. Med. Chem. 23 (2015) 2377–2386, https://doi.org/10.1016/j.bmc.2015.03.064.

[25] C. Enguehard-Gueiffier, C. Croix, M. Hervet, J.-Y. Kazock, A. Gueiffier, M. Abarbri, Convenient synthesis of alkenyl-, alkynyl-, and allenyl-substituted imidazo[1,2-*a*]pyridines *via* palladium-catalyzed cross-coupling reactions, Helv. Chim. Acta 90 (2007) 2349–2367, https://doi.org/10.1002/hlca.200790241.

[26] C. Kieffer, P. Verhaeghe, N. Primas, C. Castera-Ducros, A. Gellis, R. Rosas, S. Rault, P. Rathelot, P. Vanelle, Sonogashira cross-coupling reaction in 4-chloro-2-trichloromethylquinazoline series is possible despite a side dimerization reaction, Tetrahedron 69 (2013) 2987–2995, https://doi.org/10.1016/j.tet.2013.01.094.

[27] D. Tweats, B. Bourdin Trunz, E. Torreele, Genotoxicity profile of fexinidazole - a drug candidate in clinical development for human African trypanomiasis (sleeping sickness), Mutagenesis 27 (2012) 523–532, https://doi.org/10.1093/mutage/ges015.

[28] T.T. Wager, X. Hou, P.R. Verhoest, A. Villalobos, Moving beyond rules: the development of a central nervous system multiparameter optimization (CNS MPO) approach to enable alignment

of druglike properties, ACS Chem. Neurosci. 1 (2010) 435-449, https://doi.org/10.1021/cn100008c.

[29] T. Mosmann, Rapid colorimetric assay for cellular growth and survival: application to proliferation and cytotoxicity assays. J. Immunol. Methods 65 (1983), 55–63. https://doi.org/10.1016/0022-1759(83)90303-4.

[30] C. Zhang, S. Bourgeade Delmas, Á. Fernández Álvarez, A. Valentin, C. Hemmert, H. Gornitzka, Synthesis, characterization, and antileishmanial activity of neutral N-heterocyclic carbenes gold(I) complexes. Eur. J. Med. Chem. 143 (2018) 1635–1643. https://doi.org/10.1016/j.ejmech.2017.10.060.

[31] B. Räz, M. Iten, Y. Grether-Bühler, R. Kaminsky, R. Brun, The Alamar Blue® assay to determine drug sensitivity of African trypanosomes (*T.b. rhodesiense* and *T.b. gambiense*) *in vitro*. Acta Trop. 68 (1997) 139–147. https://doi.org/10.1016/S0001-706X(97)00079-X.

[32] T. Baltz, D. Baltz, C. Giroud, J. Crockett, Cultivation in a semi-defined medium of animal infective forms of *Trypanosoma brucei*, *T. equiperdum*, *T. evansi*, *T. rhodesiense* and *T. gambiense*. EMBO J. 4 (1985) 1273–1277. https://doi.org/10.1002/j.1460-2075.1985.tb03772.x.

[33] S. Goyard, H. Segawa, J. Gordon, M. Showalter, R. Duncan, S.J. Turco, S.M. Beverley, An *in vitro* system for developmental and genetic studies of *Leishmania donovani* phosphoglycans. Mol. Biochem. Parasitol. 130 (2003) 31–42. https://doi.org/10.1016/S0166-6851(03)00142-7.

[34] N. Greig, S. Wyllie, S. Patterson, A.H. Fairlamb, A comparative study of methylglyoxal metabolism in trypanosomatids. FEBS J. 276 (2009) 376–386. https://doi.org/10.1111/j.1742-4658.2008.06788.x.

[35] S. Wyllie, B.J. Foth, A. Kelner, A.Y. Sokolova, M. Berriman, A.H. Fairlamb, Nitroheterocyclic drug resistance mechanisms in *Trypanosoma brucei*. J. Antimicrob. Chemother. 71 (2016) 625–634. https://doi.org/10.1093/jac/dkv376.

[36] D.C. Jones, I. Hallyburton, L. Stojanovski, K.D. Read, J.A. Frearson, A.H. Fairlamb, Identification of a κ-opioid agonist as a potent and selective lead for drug development against human African trypanosomiasis. Biochem. Pharmacol. 80 (2010) 1478–1486. https://doi.org/10.1016/j.bcp.2010.07.038.

[37] M. De Méo, M. Laget, C. Di Giorgio, H. Guiraud, A. Botta, M. Castegnaro, G. Duménil, Optimization of the *Salmonella*/mammalian microsome assay for urine mutagenesis by experimental designs. Mutat. Res. Genet. Toxicol. 340 (1996) 51–65. https://doi.org/10.1016/S0165-1110(96)90039-1.

[38] H. Perdry, K.B. Gutzkow, M. Chevalier, L. Huc, G. Brunborg, E. Boutet-Robinet, Validation of Gelbond® high-throughput alkaline and Fpg-modified comet assay using a linear mixed model: validation of high-throughput comet assay. Environ. Mol. Mutagen. 59 (2018) 595–602. https://doi.org/10.1002/em.22204.

[39] C. Lecoutey, D. Hedou, T. Freret, P. Giannoni, F. Gaven, M. Since, V. Bouet, C. Ballandonne, S. Corvaisier, A. Malzert Freon, S. Mignani, T. Cresteil, M. Boulouard, S. Claeysen, C. Rochais, P. Dallemagne, Design of donecopride, a dual serotonin subtype 4 receptor

agonist/acetylcholinesterase inhibitor with potential interest for Alzheimer's disease treatment. Proc. Natl. Acad. Sci. 111 (2004) E3825–E3830. https://doi.org/10.1073/pnas.1410315111.